Final Report
for the period
November 1981 to
February 1984

Investigation of the CARS Spectrum of Carbon Monoxide at High Pressure and Temperature

July 1984

Authors:
J. H. Stufflebeam
R. J. Hall
A. C. Eckbreth

United Technologies Research Center
East Hartford, Connecticut, 06108

R83-956020-F
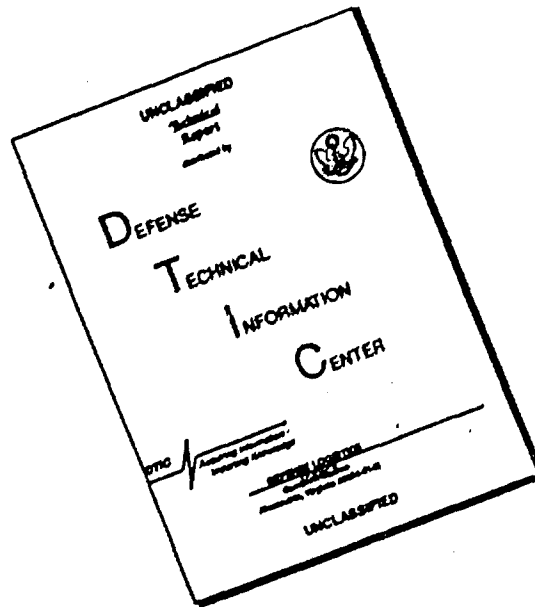F04611-82-C-0004

AD-A144 816

DTIC FILE COPY

Approved for Public Release

prepared for the: **Air Force
Rocket Propulsion
Laboratory**
Air Force Space Technology Center
Space Division, Air Force Systems Command
Edwards Air Force Base,
California 93523

84 08 21 031

DISCLAIMER NOTICE

THIS DOCUMENT IS BEST QUALITY AVAILABLE. THE COPY FURNISHED TO DTIC CONTAINED A SIGNIFICANT NUMBER OF PAGES WHICH DO NOT REPRODUCE LEGIBLY.
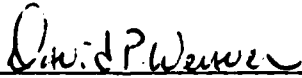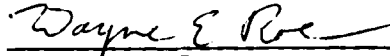
FOREWORD

This report covers research performed under Air Force contract F04611-82-C-0004 during the period November 15, 1981 to February 15, 1984. The high pressure, high temperature CARS spectrum of carbon monoxide was investigated for the end purpose of permitting accurate temperature and concentration measurements of this species in combustion media. This was accomplished by the acquisition of high quality CARS spectra under controlled laboratory conditions of temperature and pressure which were used to refine and verify a theoretical model that predicts the spectra through computer simulation. The computer model can then be used in regression analyses on experimental spectra to measure accurately the temperature and concentration of the combustion species.

The personnel involved with this contract have had responsibilities for different phases of work. John H. Stufflebeam performed the experimental investigations and acquired the CO CARS spectra; Robert J. Hall was responsible for theoretical aspects of high pressure CO CARS spectroscopy, including the computer analyses employed to model the experimintal data. Alan C. Eckbreth provided the overall direction of the experimental and theoretical aspects of this work and, in addition, supplied specific solutions to experimental problems that were encountered. This contract was monitored by David P. Weaver of AFRPL.

This report has been reviewed and is released in accordance with the distribution statement on the cover and on the DD Form 1473.
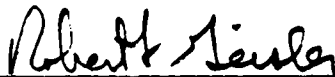

DAVID P. WEAVER
Project Manager

WAYNE E. ROE
Chief, Aerothermochemistry Branch

FOR THE DIRECTOR

ROBERT L. GEISLER
Chief, Propulsion Analysis Division

REPORT DOCUMENTATION PAGE

1a. REPORT SECURITY CLASSIFICATION		1b. RESTRICTIVE MARKINGS			
Unclassified					

2a. SECURITY CLASSIFICATION AUTHORITY	3. DISTRIBUTION/AVAILABILITY OF REPORT
	Approved for public release; Distribution Unlimited.
2b. DECLASSIFICATION/DOWNGRADING SCHEDULE	

4. PERFORMING ORGANIZATION REPORT NUMBER(S)	5. MONITORING ORGANIZATION REPORT NUMBER(S)
R83-956020-F	AFRPL-TR-84-042

6a. NAME OF PERFORMING ORGANIZATION	6b. OFFICE SYMBOL (If applicable)	7a. NAME OF MONITORING ORGANIZATION
United Technologies Research Center		Air Force Rocket Propulsion Laboratory

6c. ADDRESS (City, State and ZIP Code)	7b. ADDRESS (City, State and ZIP Code)
East Hartford, CT. 06108	AFRPL/DYCR, Stop 24 Edwards AFB, California 93523

8a. NAME OF FUNDING/SPONSORING ORGANIZATION	8b. OFFICE SYMBOL (If applicable)	9. PROCUREMENT INSTRUMENT IDENTIFICATION NUMBER
		F04611-82-C-0004

8c. ADDRESS (City, State and ZIP Code)	10. SOURCE OF FUNDING NOS.			
	PROGRAM ELEMENT NO.	PROJECT NO.	TASK NO.	WORK UNIT NO
	61102F	2308	M1	UZ

11. TITLE (Include Security Classification) Investigation of the CARS Spectrum of Carbon Monoxide at High Pressure and Temperature (U)

12. PERSONAL AUTHOR(S)
Stufflebeam, John H., Hall, Robert J., Eckbreth, Alan C.

13a. TYPE OF REPORT	13b. TIME COVERED	14. DATE OF REPORT (Yr., Mo., Day)	15. PAGE COUNT
Final Technical Report	FROM 81/11/15 TO 84/2/15	84/07	67

16. SUPPLEMENTARY NOTATION

17. COSATI CODES			18. SUBJECT TERMS (Continue on reverse if necessary and identify by block number)
FIELD	GROUP	SUB. GR.	CARS, Coherent Anti-Stokes Raman Spectroscopy, High Pressure Combustion Diagnostics, Carbon Monoxide, CARS Spectra, Collisional Narrowing, Remote Combustion Diagnostics
21	08		

19. ABSTRACT (Continue on reverse if necessary and identify by block number)

Under Contract F04611-82-C-0004 sponsored by the Air Force Rocket Propulsion Laboratory (RPL), the United Technologies Research Center (UTRC) has conducted spectroscopic investigations into the coherent anti-Stokes Raman spectroscopy (CARS) spectrum of CO. CARS is a remote laser diagnostic technique for temperature and species measurements in hostile combustion environments. As such it possesses considerable relevance to the Air Force in the general areas of ballistics and propulsion. This final report describes the results of investigations conducted into the effects of high pressure, specifically the phenomenon of collisional narrowing, on CARS spectra from which temperature and density information derive. Experimental studies of CARS spectra were conducted in carbon monoxide in a heated, high pressure cell over the range 300K-1500K,

20. DISTRIBUTION/AVAILABILITY OF ABSTRACT	21. ABSTRACT SECURITY CLASSIFICATION
UNCLASSIFIED/UNLIMITED ☐ SAME AS RPT. ☒ DTIC USERS ☐	Unclassified

22a. NAME OF RESPONSIBLE INDIVIDUAL	22b. TELEPHONE NUMBER (Include Area Code)	22c. OFFICE SYMBOL
David P. Weaver	(805) 277-5656	DYCR

DD FORM 1473, 83 APR   EDITION OF 1 JAN 73 IS OBSOLETE.

1-100 atm. The spectra were used to evaluate the UTRC CARS computer code supplied to RPL for the calculation of CO CARS frequency distributions.

R83-956020-F

Investigation of the CARS Spectrum of Carbon Monoxide
at High Pressure and Temperature

TABLE OF CONTENTS

/\

SUMMARY

Under Contract F04611-82-C-0004 sponsored by the Air Force Rocket
Propulsion Laboratory (RPL), the United Technologies Research Center (UTRC)
has conducted spectroscopic investigations into the coherent anti-Stokes
Raman spectroscopy (CARS) spectrum of CO. CARS is a remote laser diagnos-
tic technique for temperature and species measurements in hostile combus-
tion environments. As such it possesses considerable relevance to the Air
Force in the general areas of ballistics and propulsion. This final report
describes the results of investigations conducted into the effects of high
pressure, specifically the phenomenon of collisional narrowing, on CARS
spectra from which temperature and density information derive. Experimen-
tal studies of CARS spectra were conducted in carbon monoxide in a heated,
high pressure cell over the range 300K-1500K, 1-100 atm. The spectra were
used to evaluate the UTRC CARS computer code supplied to RPL for the calcu-
lation of CO CARS frequency distributions.

INTRODUCTION

High pressure combustion is extremely important in a variety of practical applications of Air Force relevance such as propulsion, airbreathing and otherwise, and ballistics. Experimental diagnostics of high pressure combustion phenomena are important to gain the understanding required to improve and control these processes. Very little is known about high pressure combustion processes due to the lack of suitable diagnostic techniques. A vast archive of data exists from insertion of thermocouples, pressure transducers, and gas sampling probes into combustion media. However, physical probes are not only confronted with survival considerations, they are of questionable utility since their presence may seriously perturb the phenomena under study. Optical techniques appear ideally suited to diagnosing such phenomena, but many are inappropriate due to poor spatial resolution, weak signal strength, etc. One optical technique, coherent anti-Stokes Raman spectroscopy or CARS, shows considerable promise for diagnosing high pressure combustion phenomena (Refs. 1,2). CARS is spatially precise (Ref. 3) and its coherent or beamlike nature is quite amenable to the limited optical apertures typical of high pressure combustion chambers. Furthermore, CARS exhibits a nonlinear dependence on molecular number density and increases rapidly in signal strength as the gas density is elevated. CARS has already been shown to be practically applicable, having been demonstrated in gas turbine combustors, internal combustion engines, propellant flames, furnaces, and shock tubes (Ref. 4 and references contained therein).

In CARS, incident laser beams at frequencies ω_1 and ω_2 (termed the pump and Stokes, respectively), interact through the third-order, nonlinear electric susceptibility, $\chi^{(3)}$, to produce the coherent CARS radiation at frequency $\omega_3 = 2\omega_1 - \omega_2$. If the frequency difference $\omega_1 - \omega_2$ coincides with a Raman-active vibrational or rotational mode of a certain species, then the CARS radiation is resonantly enhanced and uniquely characteristic of that species. In CARS, measurements of temperature are performed from the spectral shape, i.e., the CARS intensity distribution with frequency (Ref. 5). Species density can be determined from the spectral shape as well in certain concentration ranges, but, in general, density measurements are based upon the strength of the CARS signal (Ref. 6). The intensity of CARS, however, is quite linewidth dependent. Collision processes alter the spectra by perturbing the rovibronic linewidths. As the gas density increases, a variety of linewidth phenomena occur such as pressure broadening, shifting, motional or Dicke narrowing, and collisional narrowing which complicate the calculation of the CARS spectrum. For CARS, the collisional narrowing phenomenon is important for pressures above one atmosphere. Collisional narrowing occurs when adjacent Raman transitions have been pressure broadened to the extent that they overlap. The overlap allows communication between lines and they subsequently coalesce or collapse to a narrower bandwidth. Accurate modeling of high-pressure, high temperature CARS

spectra is necessary to extract temperature and density information and, thus, is fundamental to the deployment of the technique as a diagnostic. Well controlled, laboratory experiments provide numerical input to the model.

Under Air Force sponsorship, Contract F04611-82-C-0004, UTRC has investigated the phenomenon of pressure-induced, i.e. collisional, narrowing in carbon monoxide. CO CARS spectra have been obtained over the range 1-100 atm., 300K-1500K. Specific combinations of these parameters were selected for the acquisition of CARS spectra as indicated in Fig. 1. Excellent agreement in CO has been obtained between the experimental spectra and those predicted by the collisional narrowing theory.

The next section is a summary of the theoretical model of collisional narrowing and its application to the prediction of CO CARS spectra. Subsequent to that, the experimental facility is described, together with the techniques employed to obtain the high quality CO spectra. The results of this investigation are then presented and comparisons are made between the predictions from the theoretical model and the experimental spectra. Discussions of these results are included with specific reference to validation of the computer code for CO. Suggestions for future work are outlined and finally, the experimental data obtained during this investigation are contained as an attached appendix.

FIG 1

CO CARS SPECTRA PARAMETER GRID

● SPECTRA ARE INCLUDED IN APPENDIX

84-1-45-1
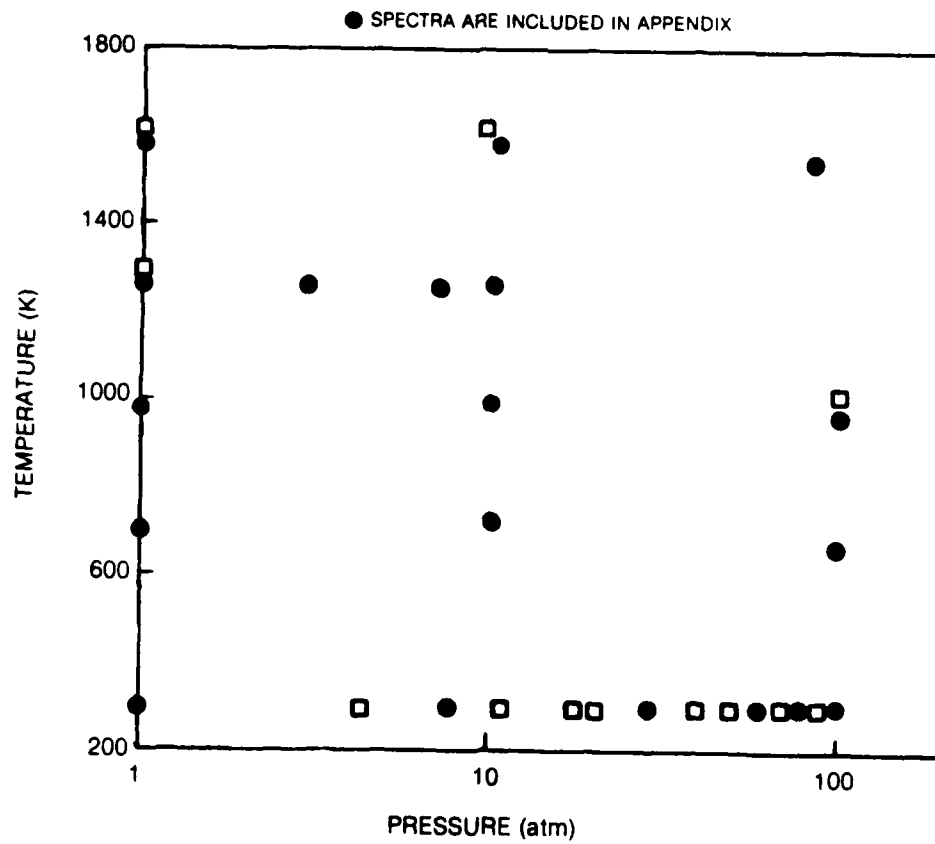
COLLISIONAL NARROWING OF CARS SPECTRA

The basic theory of CARS for the case in which none of the field frequencies encroaches upon electronic resonances in the probed molecule has been given in many publications (Refs. 1,2,7-9). It is well known that the anti-Stokes frequency is proportional to the squared modulus of the third order electric susceptibility. Since CARS temperature measurements and, in certain ranges, concentration measurements are performed from the shape of the signature (i.e. the variation of intensity with frequency), the proportionality constants are not of general interest. The third-order susceptibility can in turn be represented as a sum of frequency-dependent, complex terms associated with Raman resonances plus a nonresonant background contribution that will be essentially real and dispersionless if one and two photon resonances are avoided in all species in the mixture of interest. Of particular theoretical interest for this contract is the effect of line overlap at high pressures, which gives rise to the phenomenon of collisional narrowing. This is distinct from Dicke, or motional, narrowing wherein discrete thermal velocity groups blend together through elastic, momentum-transferring collisions. A CO vibrational Q-branch consists of many closely spaced transitions, corresponding to each rotational quantum number j that are split very slightly by vibration-rotation interaction. Different vibrational bands in CO will have a large splitting due to vibrational anharmonicity, but within each band the overlap can become very strong at modest pressures. Under such conditions, it no longer suffices to represent the resonant part of the susceptibility as a simple sum of contributions from independently broadened transitions, and very significant errors will be incurred if the effects associated with collisional narrowing are ignored.

CARS Collisional Narrowing Formalism

Generalized treatments of the collisional narrowing effect have been given by several authors (Refs. 10-12), but the analyses that are of most relevance to the present work are the extension to spontaneous Raman Q-branches by Alekseyev and Sobelmann (Ref. 13), and the extension to CARS spectroscopy of vibrational Q-branches by Hall, et.al. (Ref. 14). In the latter formulation, the resonant Raman contibution to the third order susceptibility is given in the following form:

$$\chi^{(3)} = \frac{iN}{\hbar} \sum_k \alpha_k \sum_j \alpha_j \, \Delta\rho_{jj}^{(0)} \left[G^{-1}\right]_{kj} \qquad (1)$$

where the k and j summations are over all Raman transitions; N is the probed species number density, α denotes polarizability matrix element,

$\Delta\rho_{jj}^{(o)}$ denotes the unperturbed population difference between the initial and final states in each transition, and the elements of the matrix G, which has to be inverted, are given by:

$$G_{kj} = i(\omega_k - \omega_1 + \omega_2)\delta_{kj} + \left(\frac{\Gamma_k}{2} - i\Delta_k\right)\delta_{kj} + \gamma_{kj}(1-\delta_{kj}) \qquad (2)$$

where ω_1, ω_2, and ω_k are the frequencies of the pump laser, the Stokes laser, and Raman transition Q(k), respectively; Γ_k is the Raman linewidth of transition Q(k); Δ_k is the pressure-induced shift of the transition, and δ_{kj} denotes an off-diagonal linewidth element which plays a key role in determining the extent of collisional narrowing.

Normally enough information is available to fill out the diagonal elements of the G-matrix, but the off-diagonal elements are a more complex matter. They can be represented in terms of the scattering matrix (S) for inelastic energy transfer (Refs. 13,14) and certain approximations can be introduced. For example, if vibrational energy transfer rates are slo̶ᵥ ̶ they probably are in CO, it can be shown that the off-diagonal eleme   only couple transitions with the same initial and final vibrational state   Thus, the G-matrix will be block diagonal, with one block for each vibrat: 1 band of interest. If it is also assumed that the scattering matrix is on / akly dependent on vibrational state, which means that the Raman linewidths are not dependent on vibrational band, then it can be shown that the off-diagonal element δ_{kj} is minus the first order rate coefficient for inelastic rotational energy transfer in the direction $j \rightarrow k$ (Refs. 13,14). Vibrational dephasing effects can arise from purely vibrational collisional processes and from rotational dephasing collisions if the effect of vibration-rotation interaction is significant. These effects will give rise to ordinary pressure broadening behavior even when adjacent lines are strongly overlapped, and will counteract the narrowing effect of the rotationally inelastic collisions. The rotationally inelastic collisions always contribute to the isolated linewidth, but when the pressure has increased to the point where adjacent lines are overlapped, they give rise to a narrowing of the spectrum. All the evidence is that the pure vibrational processes make small contributions to the isolated linewidths, however.

Thus, the problem of specifying the linewidth parameters which govern the narrowing process reduces, to a good approximation, to one of specifying the rotational relaxation rate matrix; this means that certain relationships such as detailed balance and S-matrix unitarity can be invoked to reduce the number of unknowns:

$$\frac{\Gamma_k}{2} = -\sum_{j\neq k} \gamma_{jk} \qquad (3)$$

6

$$\rho_{kk}^{(0)}\gamma_{jk} = \rho_{jj}^{(0)}\gamma_{kj} \qquad (4)$$

However, these relationships still do not specify the relaxation rate matrix entirely, even if one knows the diagonal, isolated linewidths. In principle, ab initio scattering calculations could be employed to generate this matrix, but there are many problems with such an approach. Accurate trajectory calculations require good intermolecular potential surfaces, and these are well known only for the most simple systems. Also, such calculations would be very time-consuming, and would have to be performed at each temperature and composition of interest. Even in the event that this could be done, it is unlikely that the results could be expressed in a succinct functional form that would facilitate their application to practical systems. For CO these rates could in principle be measured experimentally, but again, only a few such state-to-state measurements are available. The approach adopted in this program has been to exploit the considerable success enjoyed by simple, semi-empirical scaling laws in correlating rotational relaxation rate data. A good review of this field has been given by Brunner and Pritchard (Ref. 15). Typically, the state-to-state rates are given by a simple scaling law which is a function of the translational energy defect associated with the relaxation process. The most well-known laws are the exponential gap law (Ref. 16) and the inverse power law (Ref. 17). The scaling laws investigated for CO will be described in detail in the following section; next however, some simplified calculational algorithms will be discussed.

Confirmation of the basic correctness of the G-matrix approach has been given mainly by comparisons with experimental N_2 CARS spectra for pressures ranging up to 100 atmospheres (Refs. 14,17). The work of Rosasco and co-workers (Ref. 18), who used the same approach in low pressure N_2 and CO inverse Raman spectroscopy (IRS) also serves to confirm the correctness of the basic theory. One calculational difficulty associated with modelling high pressure CARS spectra is that the size of the G-matrix can become quite large, particularly at flame temperatures; because this matrix must be inverted at each frequency mesh point one selects to perform a calculation, the computer run times can become extremely long. It is desirable, therefore, to have simpler calculational algorithms. One approach useful at moderate pressures when the isolated line approximation is no longer valid is one based upon a perturbation expansion of the G-matrix as a function of pressure. In Ref. 14 it was shown how the inverse matrix could be so expanded, and the result for the first order correction to the pressure is:

$$-\frac{iN}{\hbar} \sum_k \frac{\alpha_k}{\Delta\omega_k + (i\Gamma_k/2)} \sum_{j \neq k} \frac{\gamma_{kj}\Delta\rho_{jj}^{(0)}\alpha_j}{\Delta\omega_j + (i\Gamma_j/2)} \qquad (5)$$

7

This approach was also used in Ref. (18). If one retains the second order term, then it is possible to employ the following second order perturbation expansion:

$$\chi^{(3)} = \sum_k \chi_k^{(3)} = \sum_k \bar{\chi}_k^{(3)} (1 + c_k^{(1)} + c_k^{(2)}) \qquad (6)$$

where

$$\bar{\chi}_k^{(3)} = \frac{2N}{\hbar} \, a_k^2 \, \Delta\rho_{kk}^{(0)} / (2\Delta\omega_k - i\Gamma_k) \qquad (7)$$

$$c_k^{(1)} = i \sum_{j \neq k} \frac{(2\gamma_{jk})}{2(\omega_j - \omega_k) - i\Gamma_j} \qquad (8)$$

$$c_k^{(2)} = -\sum_{j \neq k} \frac{1}{2(\omega_j - \omega_k) - i\Gamma_j} \sum_{\ell \neq j \neq k} \frac{(2\gamma_{\ell k})(2\gamma_{j\ell})}{2(\omega_\ell - \omega_k) - i\Gamma_\ell} \qquad (9)$$

It has been assumed in Eqs. 8,9 that $\omega_1 - \omega_2 \simeq \omega_k$ for any corrective terms to to be important. This perturbation expansion is particularly useful for moderate pressures in hot gases, but is not applicable over the whole range of conditions of interest in this study. It has the added advantage that it is calculationally very efficient.

Another efficient collisional narrowing algorithm that has been found to give reasonable results in N_2 is associated with Gordon's extended J-diffusion theory of rotational motion (Refs. 19-21). This simplified theory assumes strong collisions in which the magnitude and orientation of the angular momentum are randomized; there are thus no selection rules for rotational relaxation, and the probability of transfer from rotational state i to rotational state j is just proportional to the Boltzmann population of state j. In formulating the third order susceptibility for this model, it is possible to circumvent the matrix inversion step (Refs. 20-21), and the result is the very simple expression given by the following:

$$\chi_{v,v+1}^{(3)} = \frac{2N}{\hbar} \, a_{v,v+1}^{(2)} \frac{\sum_j \Delta\rho_{jj}^{(0)} / (2\Delta\omega_j - i\Gamma_j)}{1 + i \sum_j \frac{\rho_{jj}^{(0)}}{\tau_j} / (2\Delta\omega_j - i\Gamma_j)} , \qquad (10)$$

The effect of the narrowing is controlled by the simple summation term in the denominator. In addition to having some success with N_2, the rotational

8

diffusion theory has been successfully applied by Papineau and Pealat (Ref. 22) to modelling CO_2 vibrational CARS spectra at room temperature; because the vibration-rotation interaction is so small in this molecule, substantial collisional narrowing effects are encountered even at one atmosphere. The great advantage of this expression relative to the full G-matrix algorithm is its efficiency; it requires essentially no more run time than an isolated line calculation.

The UTRC high pressure code has as options these various approximations to the line overlap problem. .t.e user may specify that calculations be based upon either the isolated line approximation, the small perturbation expression, the Gordon rotational diffusion calculation, or the full G-matrix inversion.

CO Linewidth Parameters

The most fundamental parameters needed for modelling CARS spectra are the isolated linewidths, Γ_j. For CO, the Q-branch Raman linewidths are now known with great precision from the inverse Raman spectroscopy measurements of Rosasco and co-workers (Ref.18) and are shown in Fig. 2. These linewidths are in very good agreement with infrared P- and R-branch measurements by BelBruno, et. al. (Ref. 23); because the IRS measurements did not extend beyond j=20, the BelBruno P-branch linewidths were employed out to j=25 to give a set that could be used for 300K CARS calculations. BelBruno, et. al. also measured the CO vibrational overtone widths, and found only a slight temperature dependence; all of these results are an indication that it is mainly rotational relaxation that makes the dominant contribution to the linewidths. The slight band dependence of the overtone measurements may suggest a small elastic or vibrational contribution. The result that the Raman and infrared linewidths agree well is also potentially useful, because it indicates that infrared linewidth data concerning temperature and concentration dependences could be useful to fill in gaps in the Raman data.

Unfortunately, there is very little data on the temperature dependence of any of the pure CO linewidths. In general, one can express the temperature dependence in the form:

$$\Gamma_j = \rho \left(\frac{298}{T}\right)^{\eta_j} \tag{11}$$

where the temperature exponent η_j is expected to be j-dependent. Sun and Griffiths (Ref.24) state that η_j may take on values in the range 0.5 to 1.0, which presumably reflects the range expected as the interaction varies from long-range multipole to short-range, hard-sphere. Sun and Griffiths

FIT OF POWER LAWS TO Q-BRANCH LINEWIDTHS

84—1—126—1
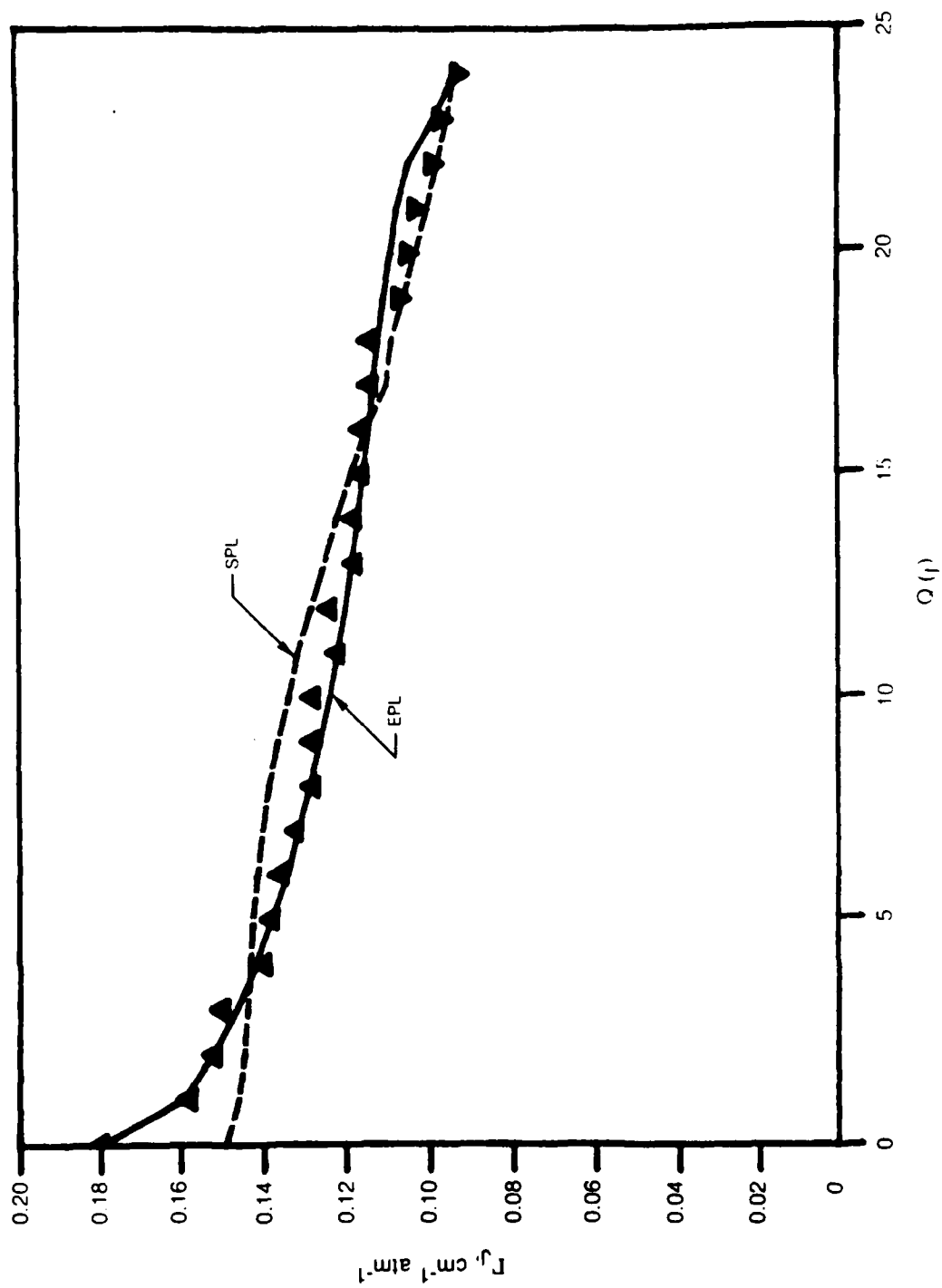
report that their measurements suggest an exponent of approximately 0.66 for lines P(25) and P(31) over the temperature range from ambient to 180 C, as opposed to the previously accepted value of approximately 0.75. However, this represents a relatively small temperature range for rotational levels that are not of great significance for low temperature CARS calculations. Varghese and Hanson (Refs. 25,26) have investigated the effect of collision partner on room temperature CO P-branch linewidths, and from measurements of these widths in a flame have made some deductions about the temperature exponent. For CO broadened by N_2, the exponent ranges from roughly 0.8 at low j to 0.5 at high j. However, none of this gives one information directly about the temperature dependences of the pure CO P-branch widths. It also seems difficult to resort to theoretical arguments to deduce how the pure broadening exponents might differ from those for N_2.

Ab initio linewidth calculations for pure CO similar to those performed successfully for pure N_2 using the theory of Bonamy and Robert (Ref. 27) would be a very useful guide, but are very time-consuming and were judged to be outside the scope of this contract. A compromise was made in which use was made of the theoretical calculations for pure N_2 Q-branch linewidths, in which to a good approximation

$$\Gamma_j \simeq p\left[AT^{-\eta_a} - BT^{-\eta_b}j\right] \qquad (12)$$

The parameters A and B were determined from a least squares fit to the room temperature data in Fig. 2, and the temperature exponents η_a and η_b were assumed, lacking better information, to be equal to those for pure N_2 (0.7 and 1.45). The η_a exponent is certainly not inconsistent with the information previously presented. The low j lines will have the strongest temperature dependence, and the high j lines will vary more slowly due to the fact that the slope decreases rapidly with temperature. Generally, the greatest sensitivity to linewidth occurs at low pressures.

With reasonable estimates for the diagonal linewidths, the off-diagonal elements can then be calculated if one assumes a particular functional form for the state-to-state rate matrix. It is likely that each molecule will represent a different situation, with no one rate model having universal applicability. In a semi-empirical fashion, the particular scaling or rate law which best satisfies all of the data on the pressure dependence must be found. There is also a choice of ways to fill out the rate matrix for a given functional form. One alternative is to assume the functional form for endothermic rates (j → k, k>j), and then use detailed balance and the conservation of probability relationships to deduce exothermic rates (j → k, k<j), in this way working down the rows of the rate matrix. The method pursued here has been to least squares fit a rate coefficient model

11

satisfying detailed balance in advance to the known isolated linewidths through the relationship:

$$\frac{\partial}{\partial c_\ell} \sum_j (\Gamma_j^{(th)} - \Gamma_j^{(exp)})^2 = 0 \qquad (13)$$

where the theoretical linewidths are given by

$$\frac{1}{2}\Gamma_j^{(th)} = -\sum_{i \neq j} \gamma_{ij} \qquad (14)$$

The isolated linewidths used in the calculation must then be identified with the theoretically-deduced values; usually there will be no problem with this because the fits are quite good.

For N_2, all of the pressure dependence data presently available indicates that a simple, population-weighted inverse power law of the form

$$\gamma_{ij} = -K_0 \rho_{ii}^{(o)} |\Delta E_{ij}|^{-\alpha} \qquad (15)$$

does a good job. The fits to the isolated linewidths are good, and the latter can be regarded as reasonably well known for N_2. This power law, hereafter referred to by the acronym SPL, gives good agreement with the IRS measurements of Ref. 18 at room temperature and modest pressures and also with UTRC spectra taken at 100 atmospheres and a temperature of approximately 1700K (Ref. 17). This model was also investigated for CO and, as will be seen, gives generally good agreement with the experiments. Another rate model that was originally proposed by Dexheimer (Ref. 28) was also investigated as part of this contract:

$$\gamma_{ij} = -K_0 (2i+1) e^{\Delta E_{ij}/2kT} |\Delta E_{ij}|^{-\alpha} e^{-b|\Delta E_{ij}|/kT} \qquad (16)$$

where the factor b is now an additional fit parameter. This is termed an exponential power law model, and will hereafter be referred to as the EPL.

The fits to the isolated linewidths obtained from these two models are also exhibited in Fig. 2. The SPL gives a generally good fit, with deviations from experiment most pronounced at low j; the disagreement here is not necessarily the result of a defect in the model because elastic contributions could be important at the smaller j values. The fit is similar to that obtained by BelBruno, et.al. (Ref. 23) who inverted their P-branch
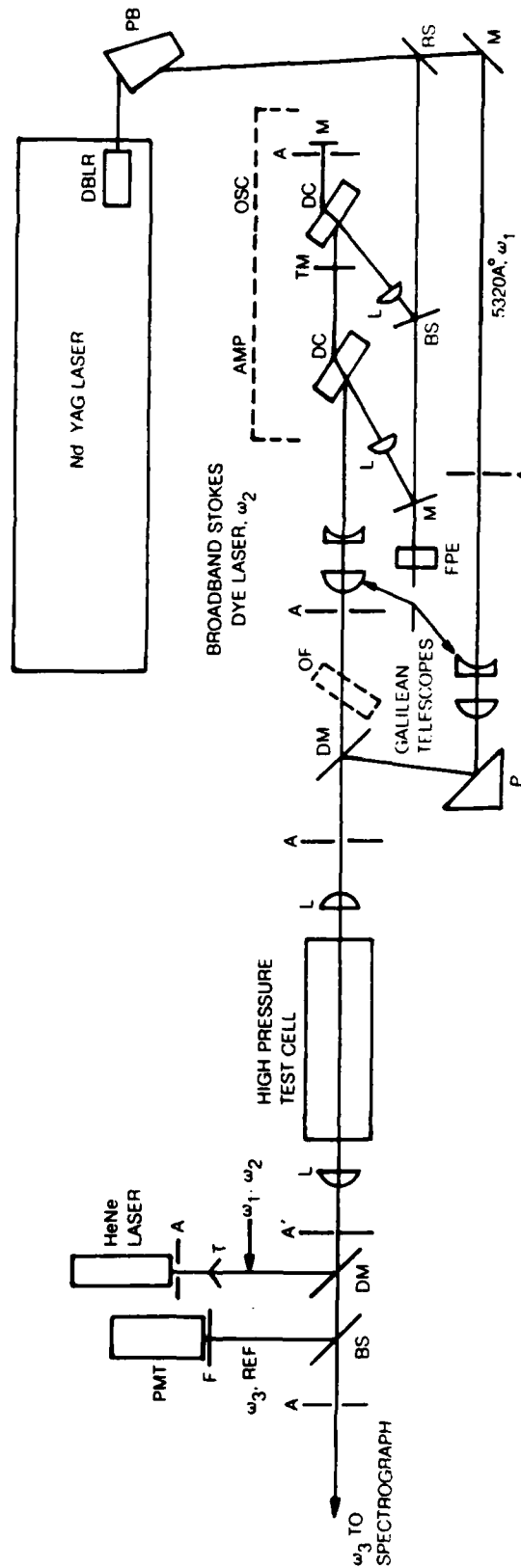
linewidths to obtain rate coefficients from a much more elaborate rate model. With the extra fitting parameter, the EPL gives a fit that is essentially perfect, as shown in Fig. 2. This does not mean that it is a better representation of the relaxation matrix, however. As will be seen, it is difficult to choose between the two models based on the high pressure data. It should be noted that the EPL does not appear to be consistent with the UTRC high temperature, high pressure data of Ref. 17.

EXPERIMENTAL APPARATUS AND TECHNIQUES

CARS Apparatus

A schematic of the apparatus used to obtain the CARS spectra is shown in Fig. 3. The output of a Quanta Ray Nd:YAG laser is frequency doubled to generate a horizontally polarized, "primary" pump beam at 5320Å (ω_1). The 10Hz laser has an average output of 2.2 Watts at 5320Å with a pulse duration of 10 nanoseconds. A beamsplitter separates 30% from ω_1 to pump the broadband Stokes dye laser oscillator and amplifier. Galilean telescopes are provided to control beam waists and the focal zone locations of ω_1 and ω_2 which are combined on the dichroic mirror and focused inside the high pressure test cell. CARS, at ω_3, is generated in the focal volume, and all three frequencies (ω_1, ω_2, ω_3) are recollimated after exiting the cell. A second dichroic mirror separates ω_3 from ω_1, ω_2 before the signal is incident on the slit of a double, one-meter monochromator with a limiting resolution of ~ 0.3 cm^{-1}. The ω_1 and ω_2 beams are trapped after reflection from the second dichroic. A He-Ne laser is shown whose output is coincident with the ω_1, ω_2 path and used for optical alignment. A beamsplitter in the ω_3 leg provides a reference signal to a photomultiplier which is used to normalize the spectrally dispersed CARS signal from the monochromator. The two signals are ratioed in a boxcar averager to account for variations in laser intensity during the scan of the CARS spectrum. At high gas pressures it is necessary to attenuate the lasers to avoid gas breakdown and stimulated Raman gain which would interfere with and perturb the CARS signal. The attenuation is achieved through a Fresnel reflection ($\sim 1.4\%$) from a flat surface. A prism is used for this purpose, as shown in Fig. 3, to avoid the back surface reflection that would result from a plane parallel element. Alternate methods of attenuation such as absorbing neutral density filters or reduction in the flashlamp energy input to the Nd:YAG laser are less desirable. They cause changes in the focal zone location due to thermal lensing in the filters or a change in divergence of the output of the Nd:YAG laser, and the focal shift can be great enough to cause damage to the sapphire rods. A Fabry-Perot etalon is included to monitor the linewidth of the primary pump beam. The convolution of ω_1 and ω_2 determine the resolution of the CARS spectra at ω_3. An angle tuned etalon option on the Nd:YAG laser results in an ω_1 linewidth of ~ 0.47 cm^{-1} and the external etalon is used to detect any shift from this value which would degrade the resolution of the CARS spectra. A vidicon detector is mounted on the spectrograph, used in the single monochromator configuration, with an overall instrument resolution of 1.1 cm which is adequate for broadband spectra. This detector can cover a broad spectral range (>200 cm^{-1}) and is used to monitor the broadband Stokes dye laser spectral position for the CO experiments. The instrument is interfaced to a PDP 11/35 computer to control its operation and store the spectral data for subsequent digital analysis. A photograph of the UTRC

FIG 3

HIGH PRESSURE, HIGH TEMPERATURE CARS FACILITY

A — APERTURE
M — MIRROR
DM — DICHROIC MIRROR
TM — PARTIALLY TRANSMITTING MIRROR
BS — BEAM SPLITTER
L — LENS
P — PRISM
PH — PELLIN BROCA PRISM

F — FILTER
DBLR — FREQUENCY DOUBLER
FPE — FABRY-PEROT ETALON
DC — DYE CELL
PMT — PHOTOMULTIPLIER TUBE
OF — OPTICAL FLAT
T — TRAP

84-1-105-2

15

FIG. 4

HIGH PRESSURE CARS FACILITY

High Pressure Facility is shown in Fig. 4 with many of the components identified that were described in the previous discussion.

High Pressure Cell

To provide well controlled conditions of temperature and pressure for the acquisition of CO CARS spectra, the high pressure vessel schematically depicted in Fig. 5 was utilized. It is a static, internally heated cell that is rated for temperatures to 1750K and pressures to 5000 psig. It is equipped with a pressure gauge, type S thermocouples, and an optical pyrometer to measure the pressure and temperature of the sample. Only the central 15 cm is heated and sapphire rods extend into the heated region to reduce thermally-induced density gradient effects in the gas. The stepped, hollow ceramic spacer, identified in the figure, is used as a target for an optical pyrometer to measure the temperature of the wall adjacent to the gas. The pyrometer reading is analytically corrected for the emissivity of the alumina and transmission through the sapphire and quartz. In the region where measurements by the thermocouple and pyrometer overlap, their temperature data exhibit a linear relationship. This linear relationship is extended to provide temperature data from the thermocouple in the region where pyrometer measurements are impossible, i.e. T < 950K.

The axial temperature profile of the cell has been measured at atmospheric pressure and the results are shown in Fig. 6. The profiles for two different central temperatures are shown. As expected, the temperature peaks in the center of the cell and smoothly decays to room temperature at the input window. Also indicated in Fig. 6 is the CARS interaction length, 70 mm, measured for the two beam BOXCARS geometry described in the next paragraph. The data show that the temperature varies only ± 3.6% over the CARS interaction length.
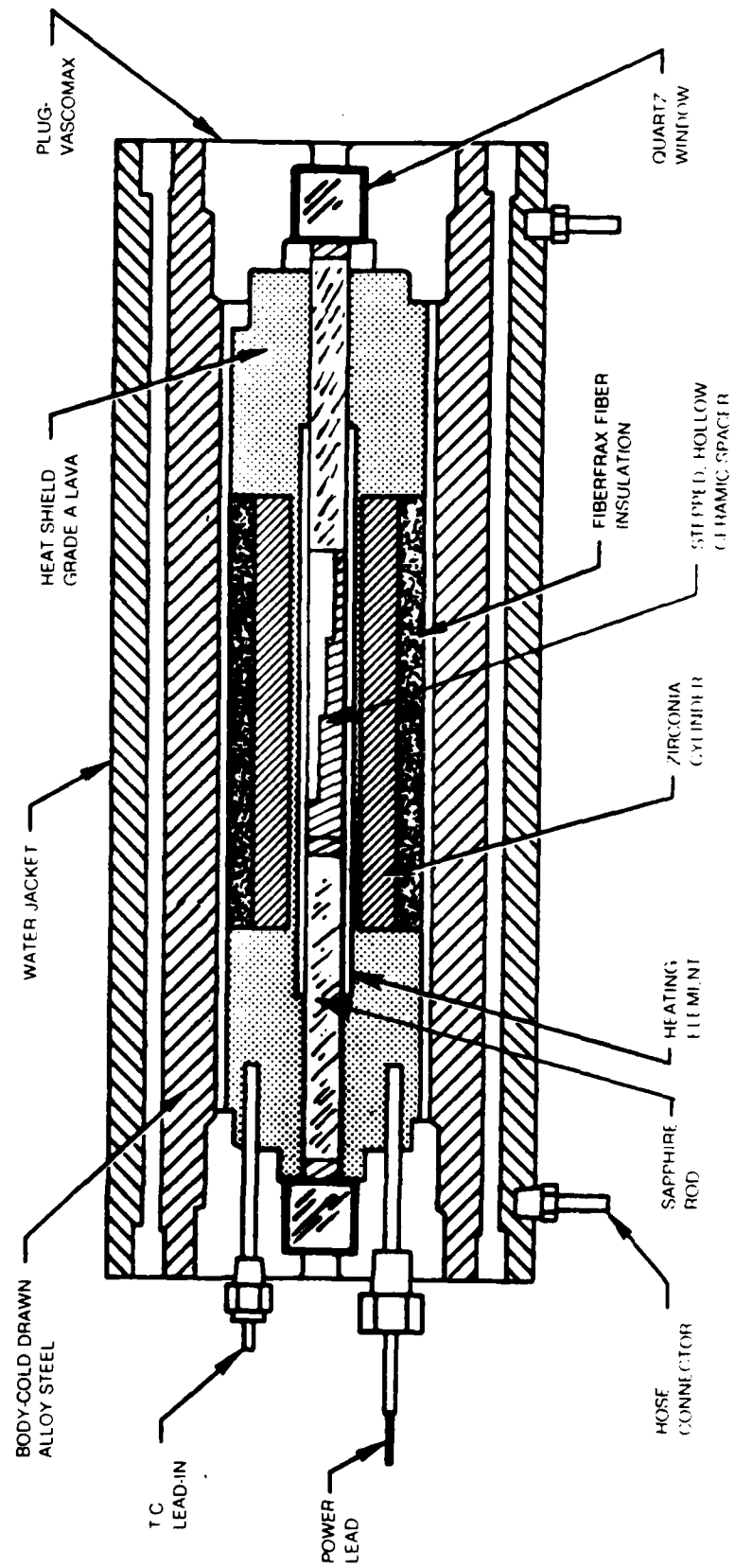
A peculiarity of the carbon monoxide molecule was encountered during this investigation. It involved the disproportionation of CO:
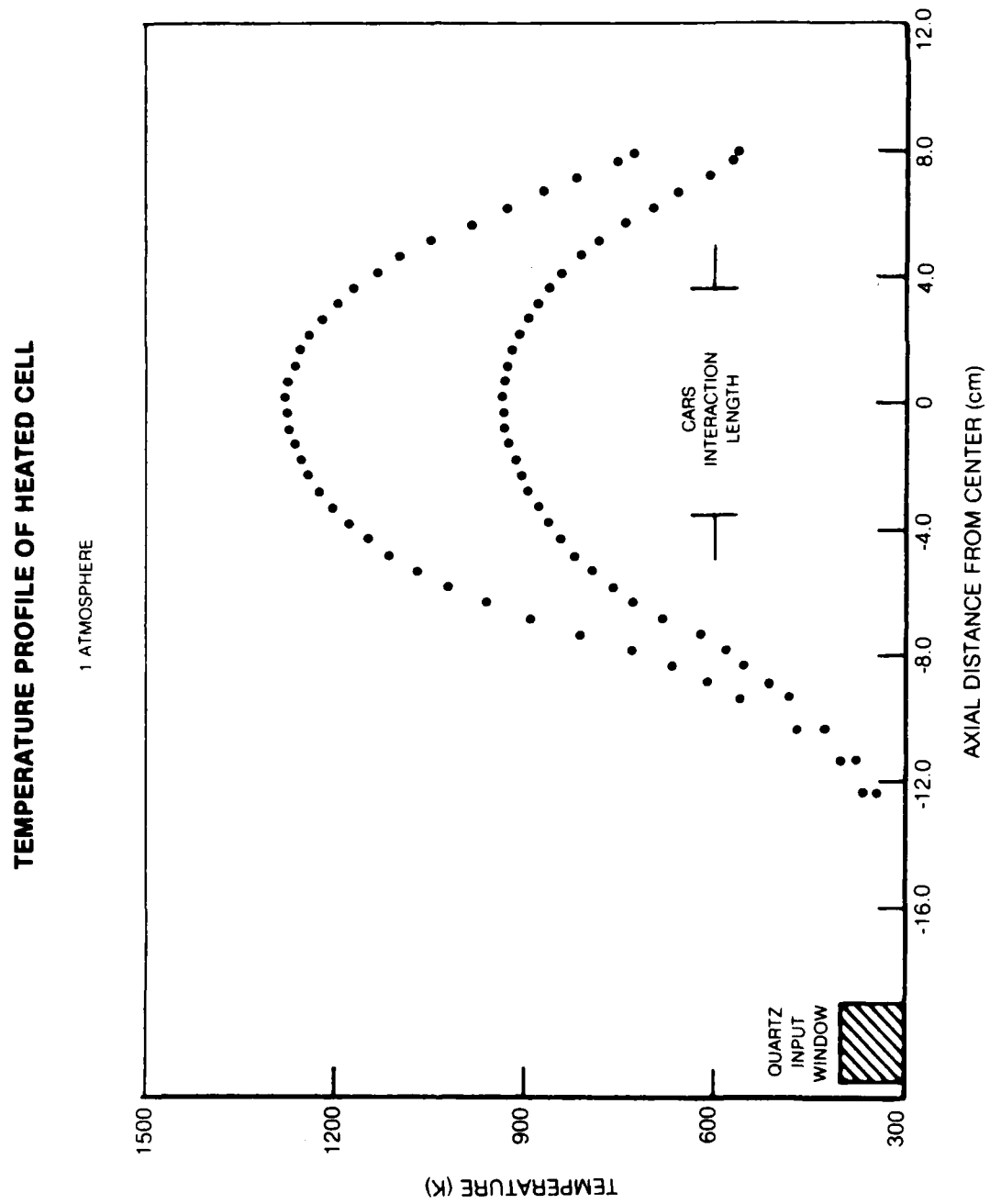
$$2CO \rightarrow CO_2 + C \qquad (17)$$

Ref. 29 indicates that this reaction is thermodynamically favored for temperatures between 700K and 1000K, in the presence of an active surface. The disproportionation was observed during the CO investigations, over the temperature range indicated and only when the sapphire rods were in the cell. This initially precluded the acquisition of CO CARS spectra above 900K because the CO decomposed to CO_2 and carbon. The carbon coated out on the faces of the rods which caused absorption and attenuation of the pump lasers so that no CARS could be generated. This result was verified by SIMS (Secondary Ion Mass Spectroscopy) analysis of the deposits on the sapphire rods. After considerable experimental effort and collaboration, the simple solution was to heat the cell to the desired temperature at 1 atm.

INTERNALLY HEATED PRESSURE VESSEL FOR CARS DIAGNOSTICS

PLUG-VASCOMAX

QUARTZ WINDOW

HEAT SHIELD GRADE A LAVA

FIBERFRAX FIBER INSULATION

STEPPED, HOLLOW CERAMIC SPACER

WATER JACKET

ZIRCONIA CYLINDER

BODY-COLD DRAWN ALLOY STEEL

HEATING ELEMENT

SAPPHIRE ROD

TC LEAD-IN

POWER LEAD

HOSE CONNECTOR

83-1-4-2

18

TEMPERATURE PROFILE OF HEATED CELL

1 ATMOSPHERE

84-1-105-1

pressure, then fill the hot cell to the pressure desired for the CARS
spectra and wait ~30 minutes for the gas to equilibrate. Some dispropor-
tionation still occurred but not at the spatial location of the CARS sample
volume. The center of the cell was above the disproportionation tempera-
ture so the ends of the rods remained relatively clear which allowed ac-
quisition of the high pressure, high temperature spectra. Inspection of
the rods after this exercise revealed a band of soot approximately 3 cm
from the end of the sapphire rods – apparently the location of the optimum
temperature for disproportionation.

Phase Matching Approaches

The limited optical access provided by the test cell dictates either a
coaxial alignment, or tightly packed BOXCARS geometry, of the pump and
Stokes lasers used to generate CARS. Acquisition of CO spectra at room
temperature or at elevated temperatures above 10 atm. pressure employed a
two beam, three dimensional phase-matching configuration called USED CARS
(Ref. 30). In this two beam approach, the ω_2 Stokes beam is coaxial with
and inside the annular ω_1 pump beam. The annular pump results from the
unstable resonator employed on the Nd:YAG laser. The pump and Stokes beams
do not overlap until the focal region where the pump beam transforms or
fills in. The resulting resolution elememnt is a cylinder of 0.1 mm diame-
ter and 100 mm long. For 295K spectra there are no thermal gradients to
complicate interpretation of the spectra and this resolution is adequate.
In the high pressure, high temperature experiments, (P > 10 atm.), thermal
gradients cause refractive index changes in the gas which steer the laser
beams to the extent they cannot be propagated through the cell. Turbulence
is also created in the gas and destroys the spatial coherence of the pump
beams which inhibits the generation of CARS. These effects are reduced
significantly by the insertion of sapphire rods and high quality CARS
spectra are observed. The presence of the sapphire rods also improves the
axial resolution by limiting the gas sample to 51 mm in length. The sap-
phire rods were not used for the spectra at pressures from 1 to 10 atm.
and elevated temperatures because pump beam intensities that would damage
the rods were required to obtain high quality spectra. In this case the
best axial resolution is achieved with a two beam BOXCARS arrangement
(Ref. 31) in which the Stokes beam is located on the circumference at one
side of the annular ω_1 pump beam. The measured axial interaction length
for this case is 70 mm.

The two beam BOXCARS geometry is implemented with an optical flat,
shown in Fig. 3, that is inserted after the Stokes beam amplifier to dis-
place ω_2 to the edge of ω_1. The BOXCARS formed in this geometry is spa-
tially filtered from the pump and Stokes beams as well as from any collin-
early phase matched contributions to ω_3 since the collinear contributions
will have poor axial resolution. An added benefit in this geometry is that
less ω_1 is incident on the slit of the monochromator because of the spa-
tial filtering. This reduces the noise component of the monochromator out-
put and results in higher quality spectra.

RESULTS AND DISCUSSION

Experimental Results

CARS spectra of carbon monoxide were acquired over the range 300K –
1500K, 1 – 100 atm., using the experimental facility and techniques de-
scribed above. A more descriptive synopsis of the actual parameters inves-
tigated is shown in Fig. 1 and the CO spectra themselves are included in
the appendix of this report.

Comparison of Theory and Experiment

The starting point for modelling the experimental spectra is the 295K
spectrum at one atmosphere pressure, as given in Fig. 7. It is apparent
that all of the theoretical approaches reproduce this spectrum, although
the EPL does have a tendency to predict more narrowing than is observed.
As will be seen, this is the case in most of the high pressure spectra.
The Gordon model gives results so close to the isolated line and SPL pre-
diction that it is not shown in Fig. 7. It is clear that there is no mod-
elling problem associated with the 295K data at one atmosphere.

There is a small problem associated with modelling the hot CO spectra
at one atmosphere, however, with diagreement found in the spectral vicinity
of the fundamental bandhead. An example is shown in Fig. 8, which shows the
observed pure CO spectrum at one atmosphere and a measured temperature of
1265K. The somewhat surprising feature of the spectrum is the prominent
feature near the fundamental bandhead; the rest of the spectrum shows the
expected Q-branch features on the hot side of the fundamental, as well as
the hot band with no unusual features. As the Appendix shows, this band-
head shape is seen in all the hot spectra. Theoretical calculations using
the baseline Raman linewidths do not predict that this feature should be as
significant as it appears to be experimentally, although there is a small
theoretical peak at this spectral location, Fig. 9. Theoretically, this
peak seems to arise both from the ordinary cross-terms interference typical
of CARS (that is, an isolated line calculation predicts it), and from col-
lisional narrowing effects. It is stronger, when as in Fig. 9, collisional
narrowing is included using the EPL model. If the Raman linewidths in the
vicinity of the bandhead are increased by assuming a temperature exponent
equal to 0.5 instead of 0.7, the theoretically predicted feature does be-
come more prominent, as shown in Fig. 9, but is still in disagreement with
experiment. If the temperature exponent is set equal to zero, it is clear
that a much stronger feature is predicted. Choosing a temperature exponent
between zero and 0.5 would probably resolve the discrepancy, but this would
be physically unrealistic. This temperature dependence would then become
inconsistent with what P-branch data are available, and does not seem theo-
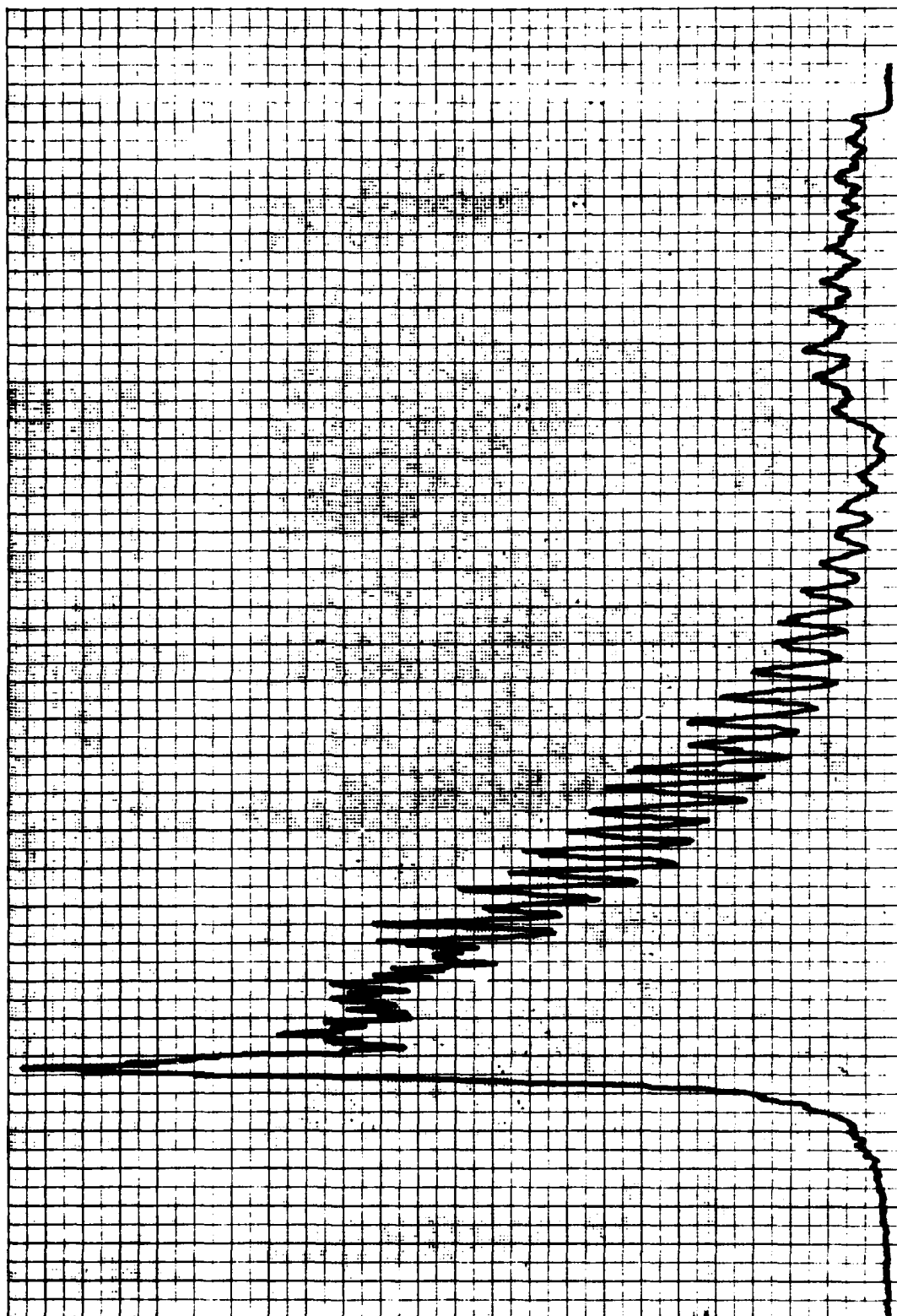retically justifiable. The j-dependence of the linewidths is so weak at

FIG. 7

COMPARISON BETWEEN THEORY AND EXPERIMENT — CO CARS
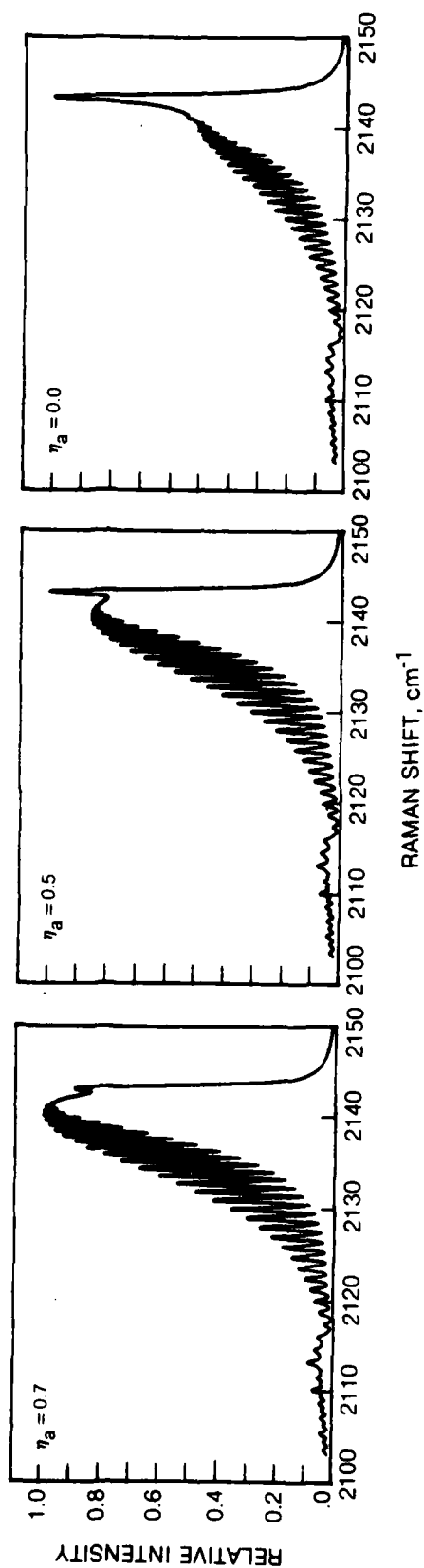
T = 295K   P = 1 0 atm

OVERALL RESOLUTION = 0 47 cm^{-1}

84—1—45—6

22

FIG 8
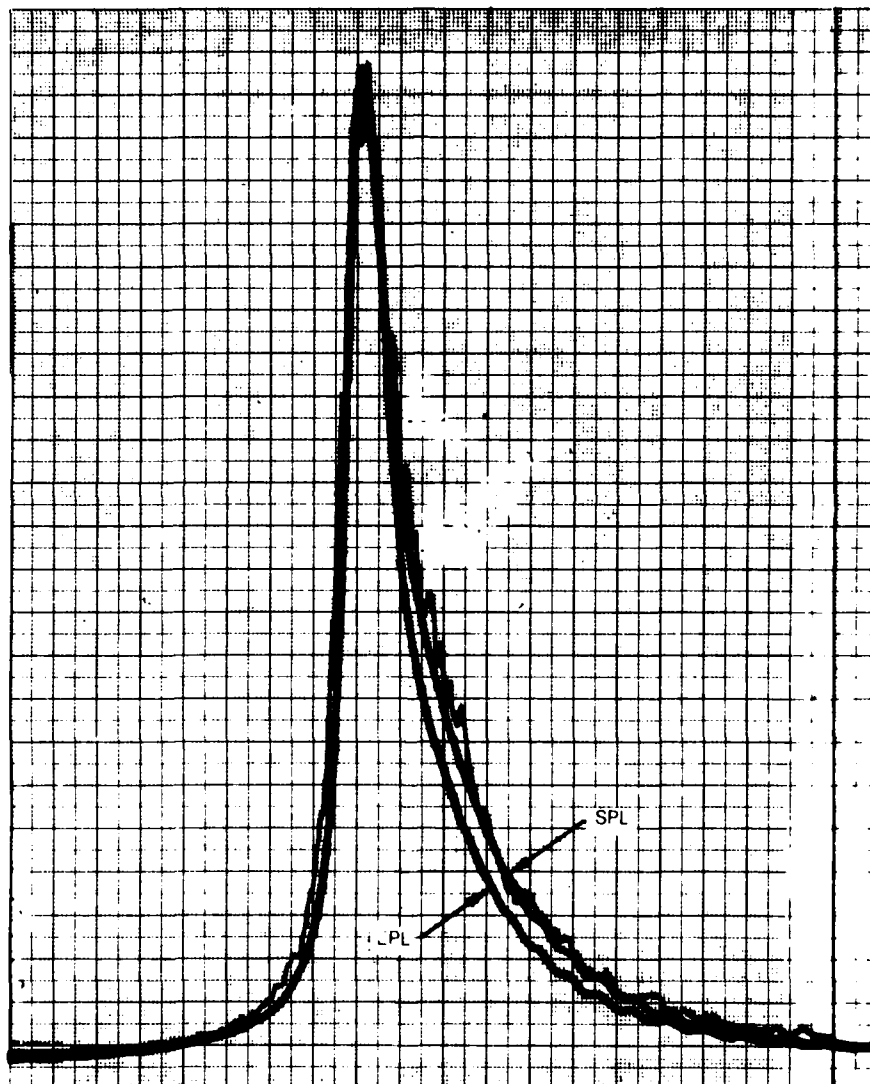
EXPERIMENTAL CO CARS SPECTRUM

T = 1265 K   P = 1 0 atm

OVERALL RESOLUTION = 0 47 cm^{-1}

84—1—45—3

23

FIG. 9

PREDICTED SENSITIVITY OF CO CARS SPECTRUM TO LINEWIDTH TEMPERATURE DEPENDENCE

$T = 1265°K$ $p = 1$ atm   RESOLUTION 0.4 / cm^{-1}

high temperature that this does not seem to be a sensitive parameter. As will be seen, collisional narrowing calculations at higher pressure are in reasonable agreement with experiment, and thus it does not seem likely that the fault lies with the collisional narrowing models. For a given rate law model, the question of the proper temperature dependence loses importance as the pressure is increased because the calculations lose sensitivity to isolated linewidth.

One possibility that should be considered is the linewidth augmentation effect suggested by St. Peters (Ref.32). He argues that the Raman linewidths are effectively increased by the sum of the finite axial mode widths in the pump and Stokes lasers. That is, he asserts that the effective linewidth which goes into the third order susceptibility calculation is $\Gamma = \Gamma_j + \Gamma_p + \Gamma_s$, assuming that all of the modes in the broadband pump and Stokes have roughly the same widths. This argument is tempting because there is speculation that the Stokes modal widths might be as much as .05 cm^{-1}, which is the kind of number that is needed to resolve the discrepancies discussed above. This explanation is also consistent with the data at high pressure, and if it were true would have very significant implications because the linewidth at low pressure would then become an instrumental feature and not a function of medium conditions. This argument is being raised here only as a possibility. It is questionable however, because it does not need to be invoked in the case of N_2 spectra obtained from the same apparatus where the observed interference at the bandhead is significantly smaller.

Another possibility concerns the longitudinal temperature gradients which are known to exist at high temperatures (Fig. 6). In propagation through such gradients, each Fourier component of the anti-Stokes field will be given by a coherent superposition of the contributions from a volume at each temperature along the path; thus, interference effects will occur that might be exaggerated by the different temperature weightings assigned to the susceptibily at each location. The bandhead has been seen to be quite sensitive to such interference effects. However, the problem with this argument is that the measured gradients are not severe, as can be seen in Fig. 6. Certainly no ambient CO contributions are being mixed in, nor is the bandhead spike predicted at the lowest temperature prevailing in the interaction region, and an incoherent superposition of spectra with temperatures within the interaction length do not show the interference at the bandhead. There is the problem too of reconciling this with the good fits obtained at higher pressure. Although the gradients might become smaller, temperature distributions at high pressure have yet to be determined.

Thus, the interference feature which is observed at one atmosphere in the hot spectra is still something that is not entirely understood, and there does not seem to be a completely satisfactory explanation for it at the present time. In any event, the failure of the theory to account for it does not necessarily have negative implications for diagnostics. The

theory and experiment agree well in all other parts of the spectrum, so that regression analyses will yield accurate temperature predictions, and measurements that rely on the total signal strength (i.e. the integrated area of the spectrum), will be little affected by the narrow interference feature at the bandhead.

The pressure dependence of the 295K spectra has previously been compared to the predictions of the SPL and the Gordon model (Ref.17). These results are shown in Fig. 10. Both these models require an average elastic dephasing contribution of about 5% of each isolated linewidth to be consistent with the data at high pressures. In reality, it is likely that the elastic contributions would have a j-dependence, like the isolated linewidths. Based on the results of Koszykowski (Ref. 33) it would be reasonable to expect that the elastic contributions would be most important for the low j-values, with diminishing importance as j increases. The calculated results for the EPL model at one hundred atmospheres are shown in Fig. 11. As can be seen, the agreement is impressive, although it too would require some pure broadening (elastic) contributions to make the fit perfect (the experimental bandwidth is 1.58 cm^{-1}, the theoretical bandwidth is 1.35 cm^{-1}).

In Figs. 12-20 theory-experiment comparisons are presented for conditions which represent the range of the experimental investigations. Theoretical overlays corresponding to both the SPL and EPL are presented; for the hot calculations at modest pressures, the perturbation expansion Eq. 6 was employed; for pressures in the vicinity of 100 atmospheres, the full G-matrix inversion was necessary. There may be a general tendency for the EPL model to overpredict the extent of narrowing; the exception is Fig. 20, where it seems to give a better fit than the SPL. On the other hand, there are certain spectra where the SPL does not predict quite enough narrowing. Nevertheless, these defects are small, particularly when one considers the enormous errors that would be incurred by neglect of narrowing entirely (Figs. 18,20). It seems reasonable to conclude that both models do quite well. The Gordon model predictions are, in general, slightly less satisfactory than those of the simple power law. As an example, Fig.16 compares a prediction of the Gordon model with those of the power laws at 104 atmospheres and 645 K. Elastic contributions were not included in any of the hot spectra; the hot N_2 calculations discussed earlier indicated no need for such contributions in that molecule. As discussed earlier, the question of the proper temperature dependence of the linewidths becomes moot at higher pressures; numerical tests for the hot, high pressure spectra (Figs. 18, 20) showed no significant sensitivity to linewidth for each model.

The results of these comparisons suggest that it might be desirable to consider a rate law which combines the SPL and EPL in some way. The problems in the fundamental bandhead of hot, low pressure spectra also are a question that should be addressed. It might be useful in this regard to undertake ab initio calculations of the kind that have been performed for
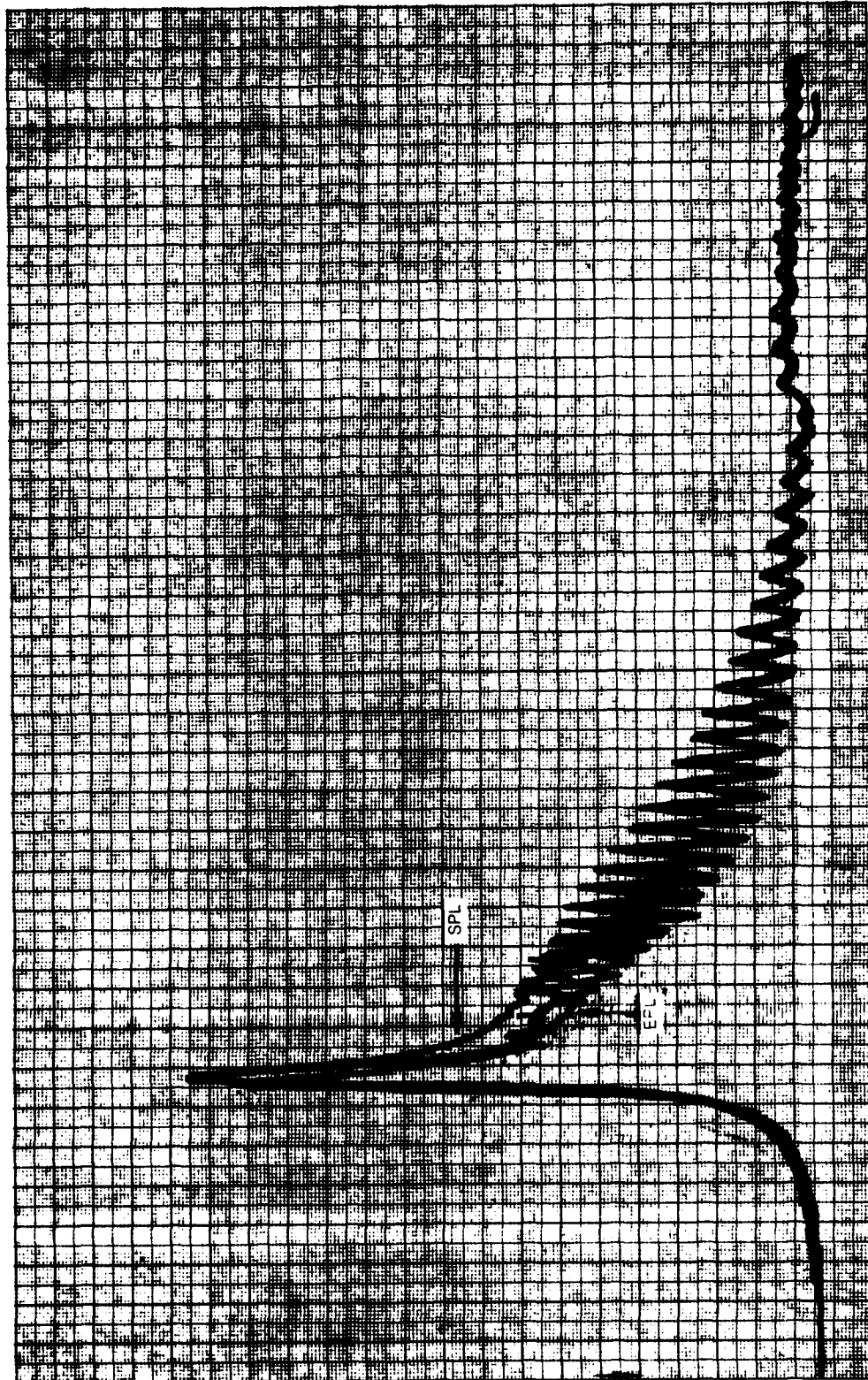
FIG. 10

CO BANDWIDTH VS PRESSURE AT ROOM TEMPERATURE

OVERALL RESOLUTION = 0.47 cm^{-1}

84-1-45-2

FIG. 11
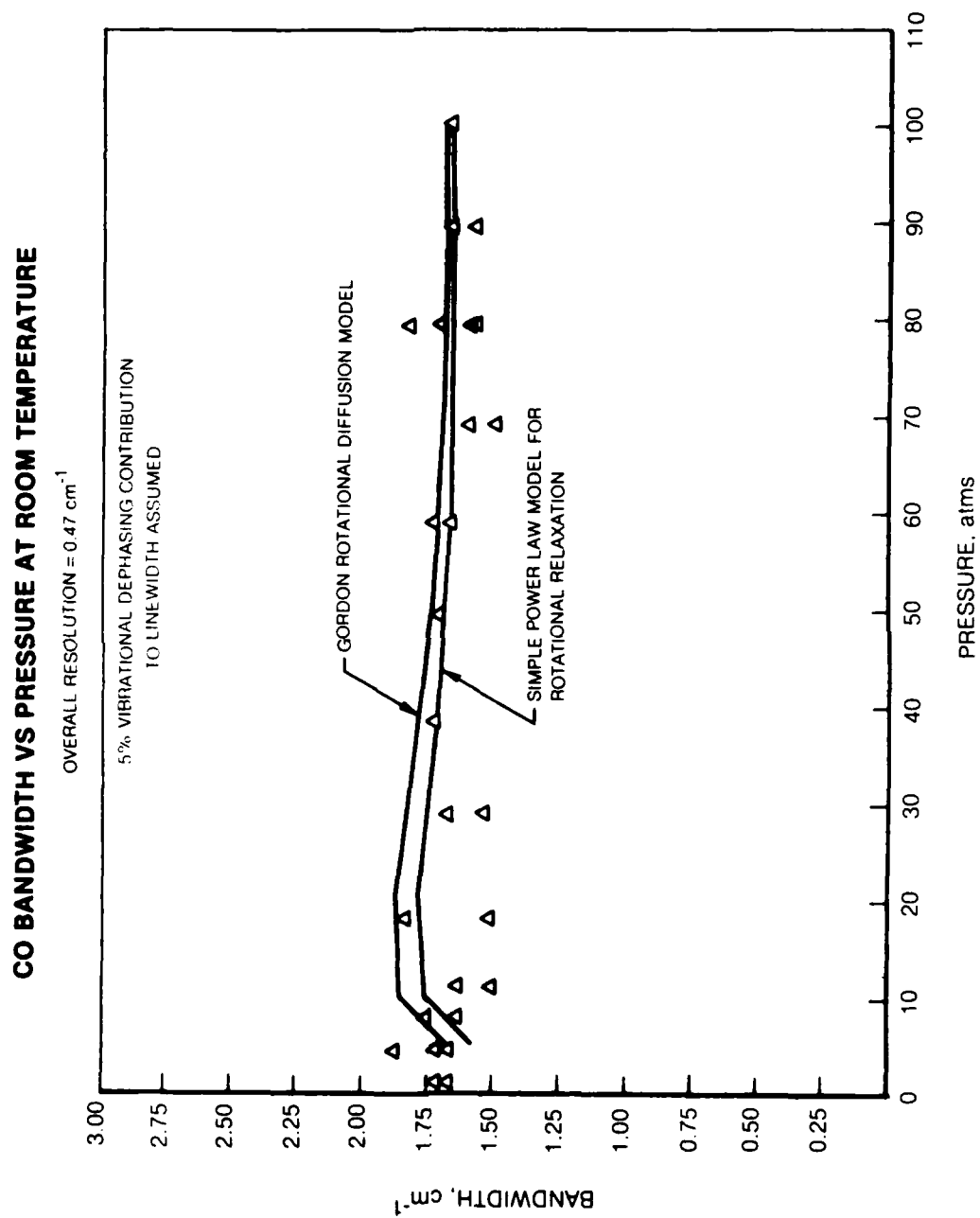
COMPARISON BETWEEN THEORY AND EXPERIMENT — CO CARS

T = 295K   P = 100.3 atm

OVERALL RESOLUTION = 0.47 cm^{-1}
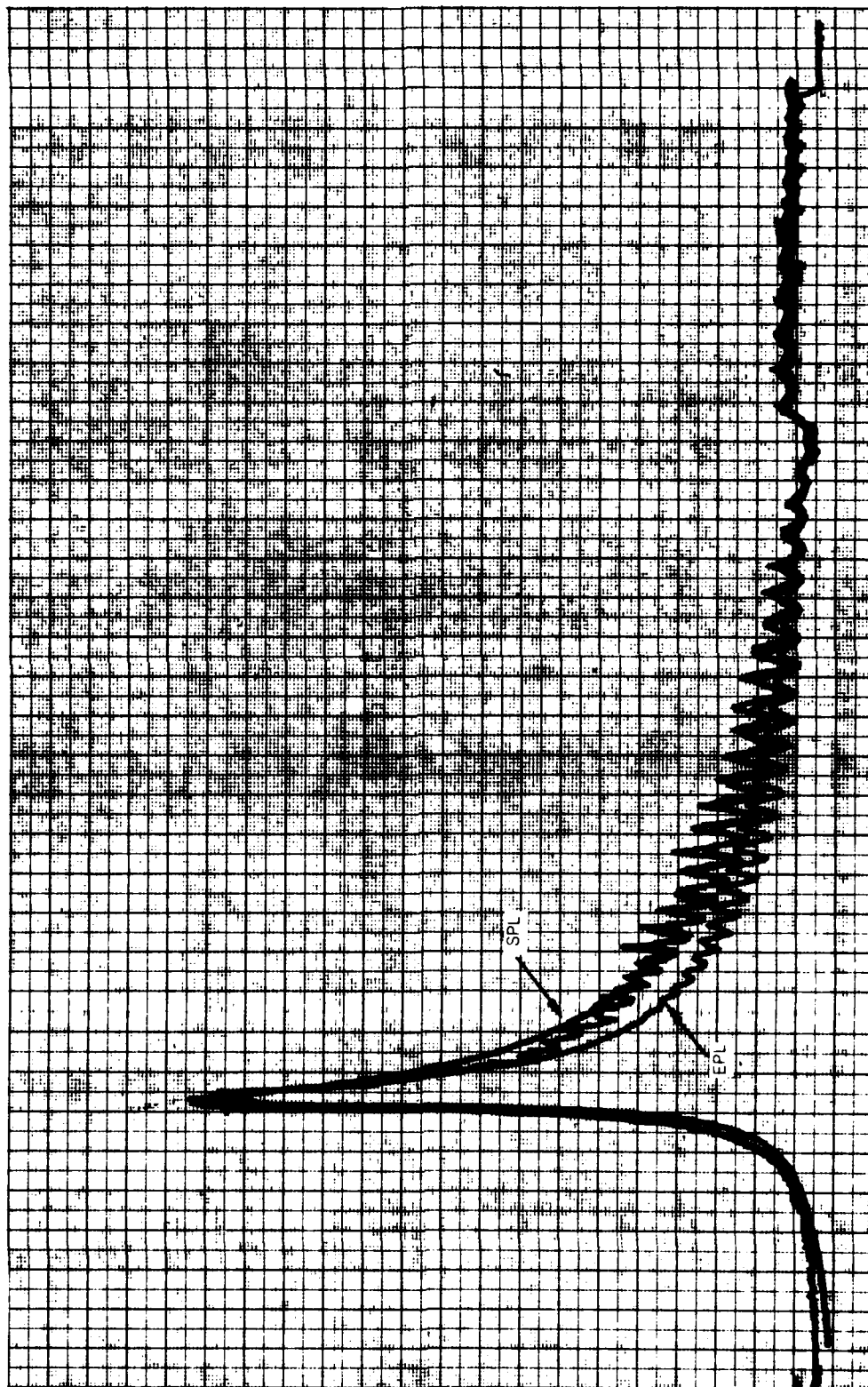
28

FIG. 12
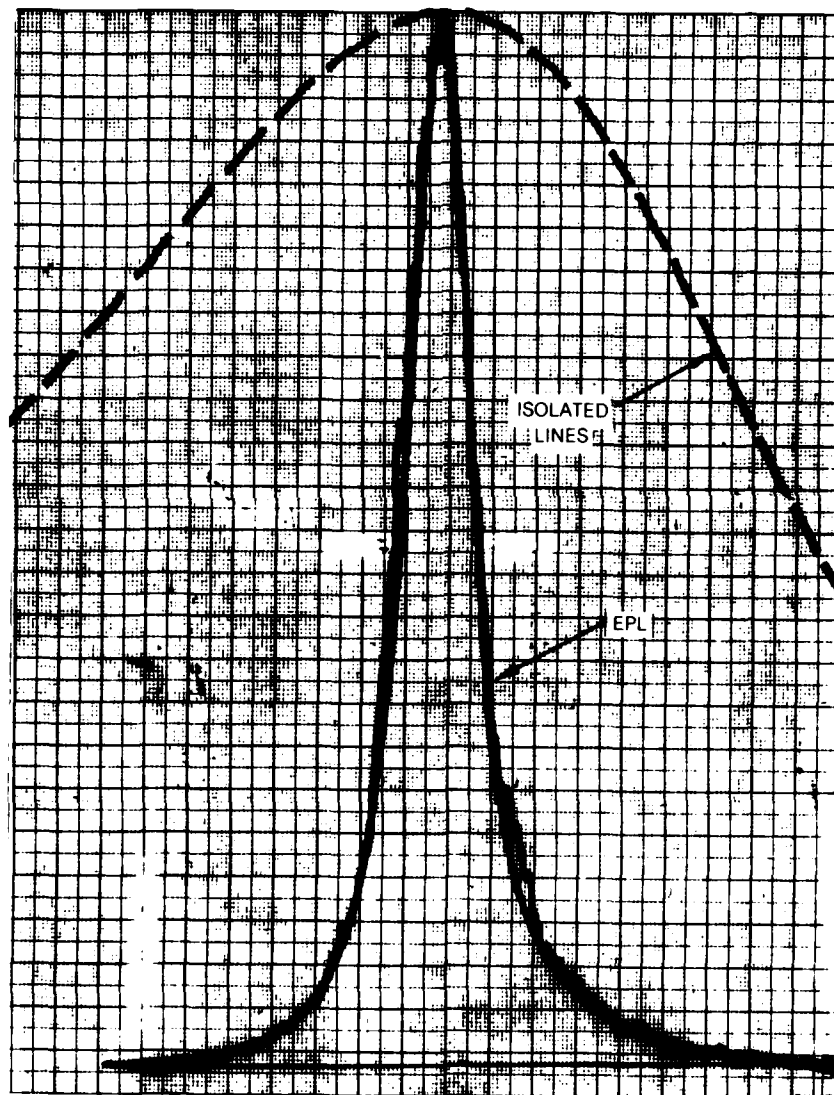
COMPARISON BETWEEN THEORY AND EXPERIMENT — CO CARS

T = 1256K   P = 3.0 atm

OVERALL RESOLUTION = 0.47 cm⁻¹
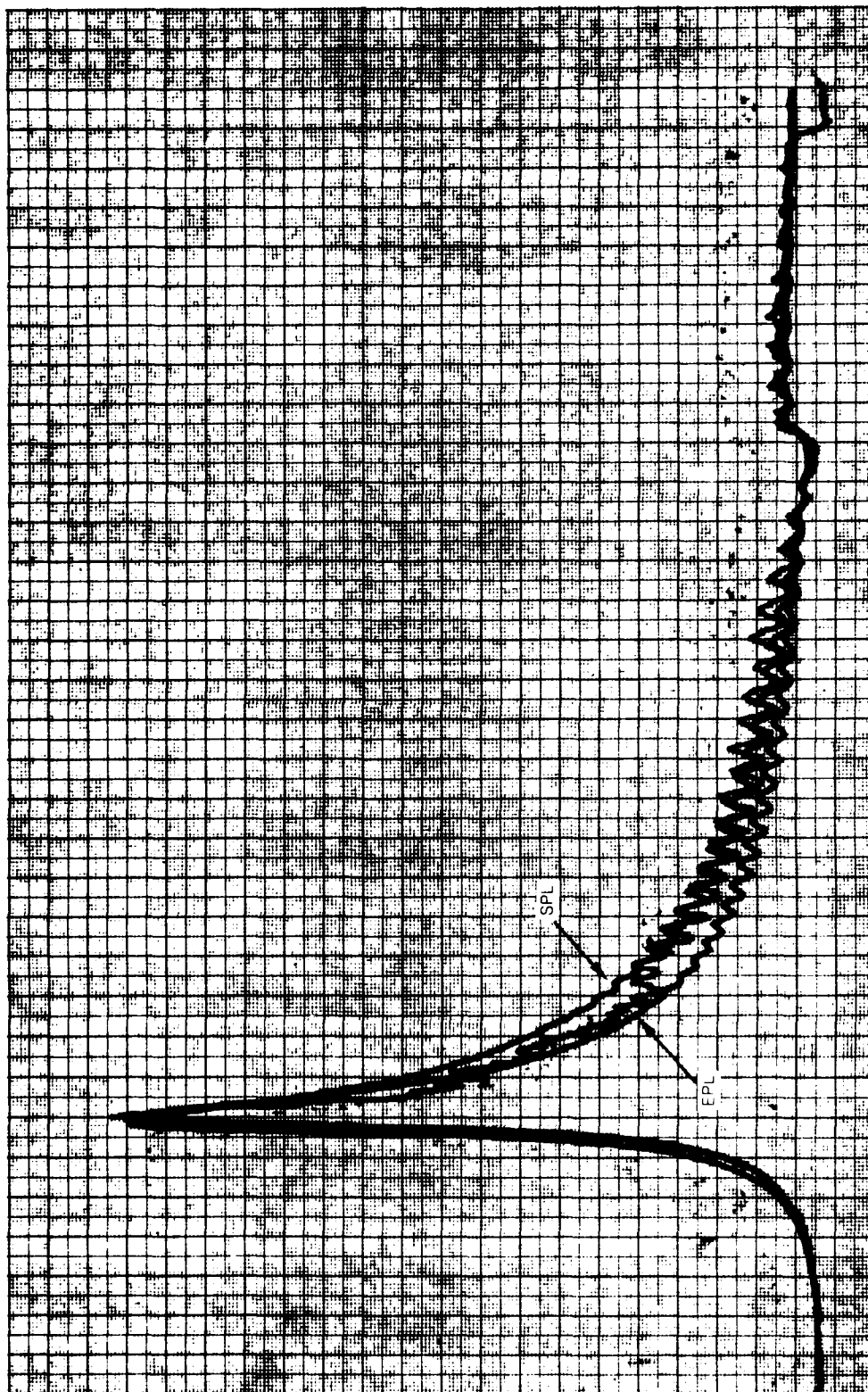
84—1—45—8

FIG. 13

COMPARISON BETWEEN THEORY AND EXPERIMENT — CO CARS

T = 1247K   P = 7.1 atm

OVERALL RESOLUTION = 0.47 cm^{-1}

SPL

EPL

84—1—45—7

COMPARISON BETWEEN THEORY AND EXPERIMENT — CO CARS

T = 1250K   P = 10 2 atm
OVERALL RESOLUTION = 0 47 cm⁻¹

SPL

EPL

FIG. 15

COMPARISON BETWEEN THEORY AND EXPERIMENT — CO CARS

T = 736K   P = 10 2 atm

OVERALL RESOLUTION = 0 47 cm⁻¹

SPL

EPL

84-1-46-13

R83-956020-F

FIG. 16
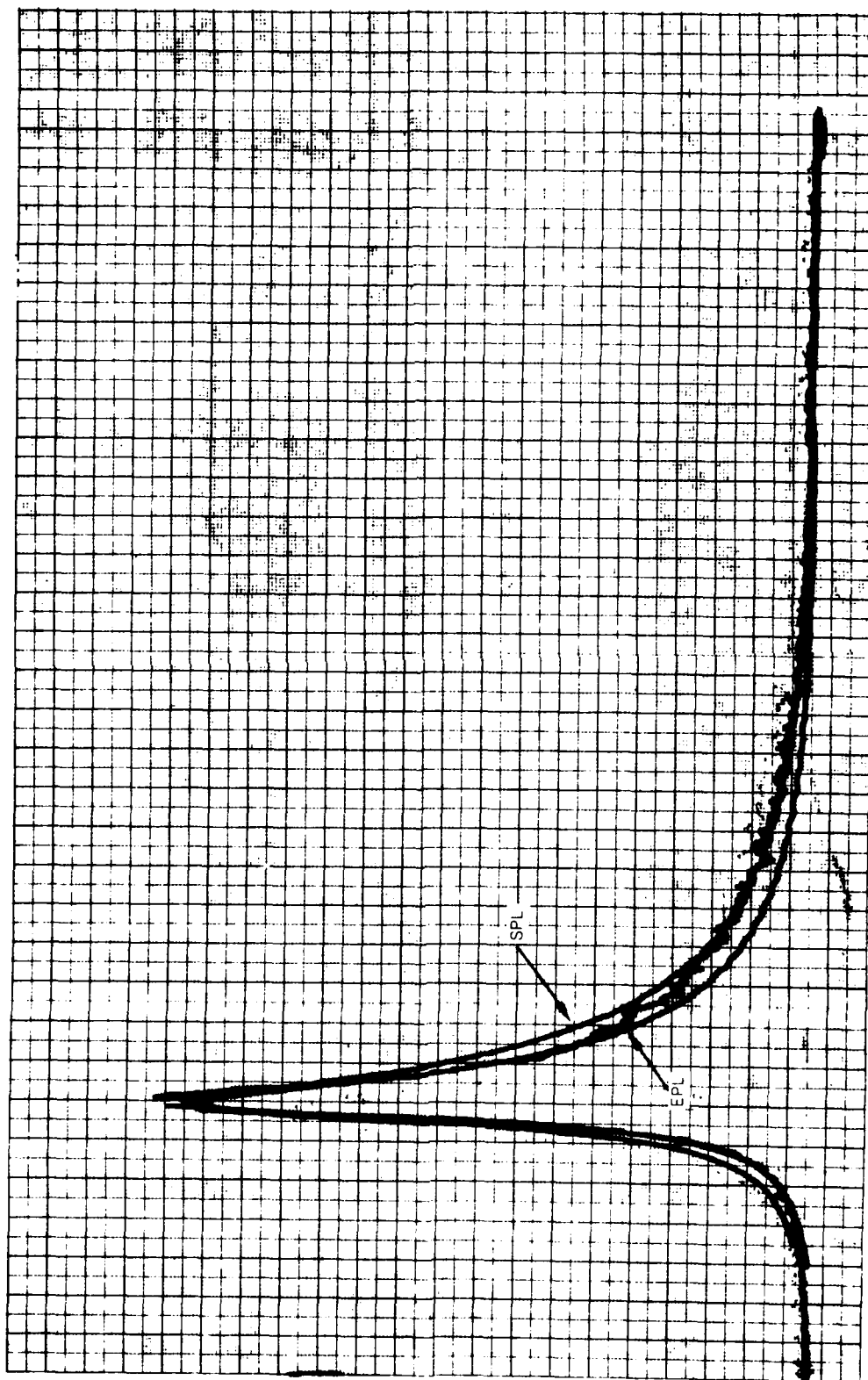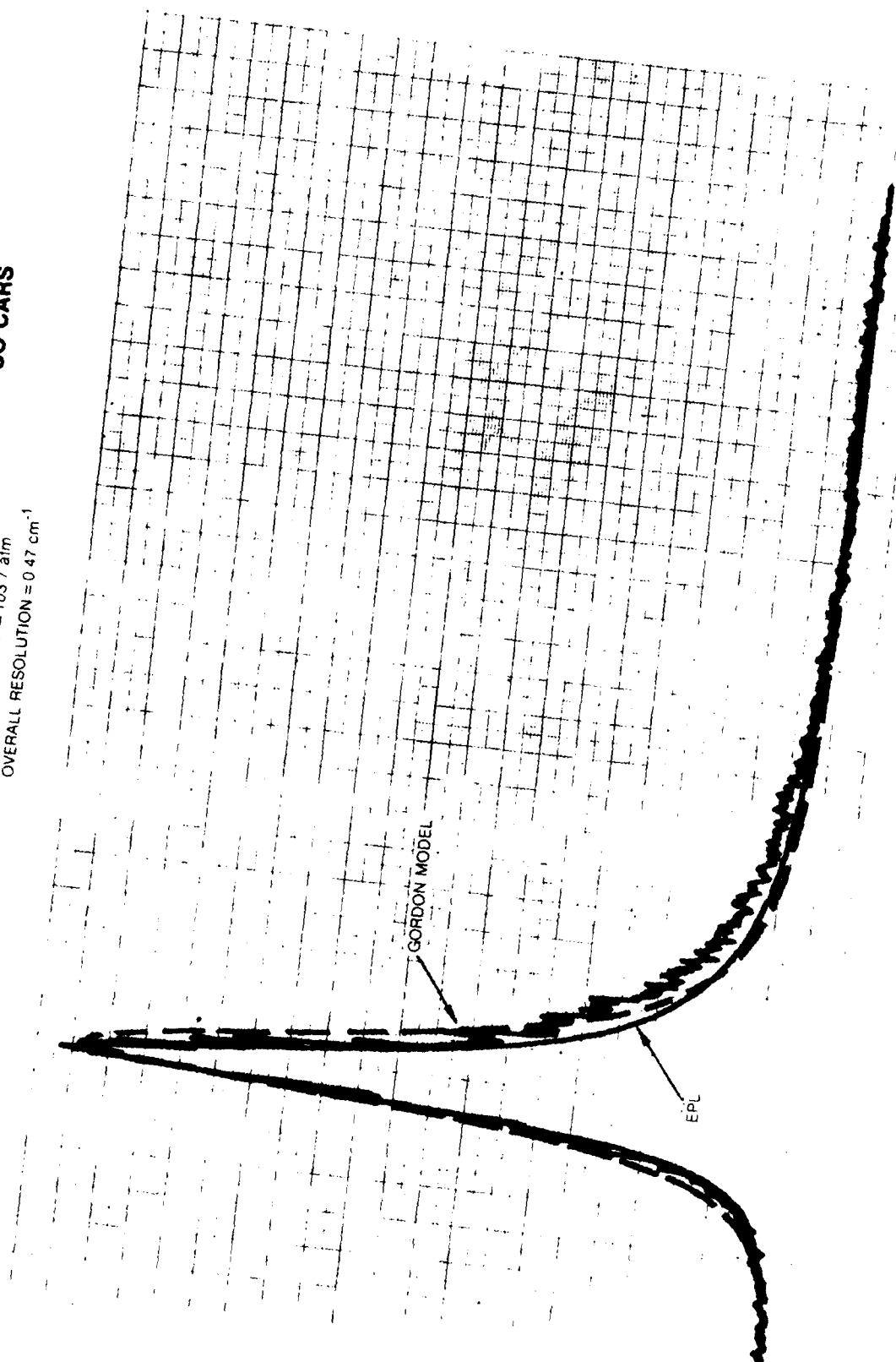

COMPARISON BETWEEN THEORY AND EXPERIMENT — CO CARS

$T = 645K$ $P = 103\ 7\ atm$
OVERALL RESOLUTION $= 0\ 47\ cm^{-1}$

GORDON MODEL

EPL

84-1-45-11

FIG. 17

COMPARISON BETWEEN THEORY AND EXPERIMENT — CO CARS

T = 971 K   P = 9.8 atm

OVERALL RESOLUTION = 0.47 cm^{-1}

SPL

EPL

84—1—45—14

FIG. 18
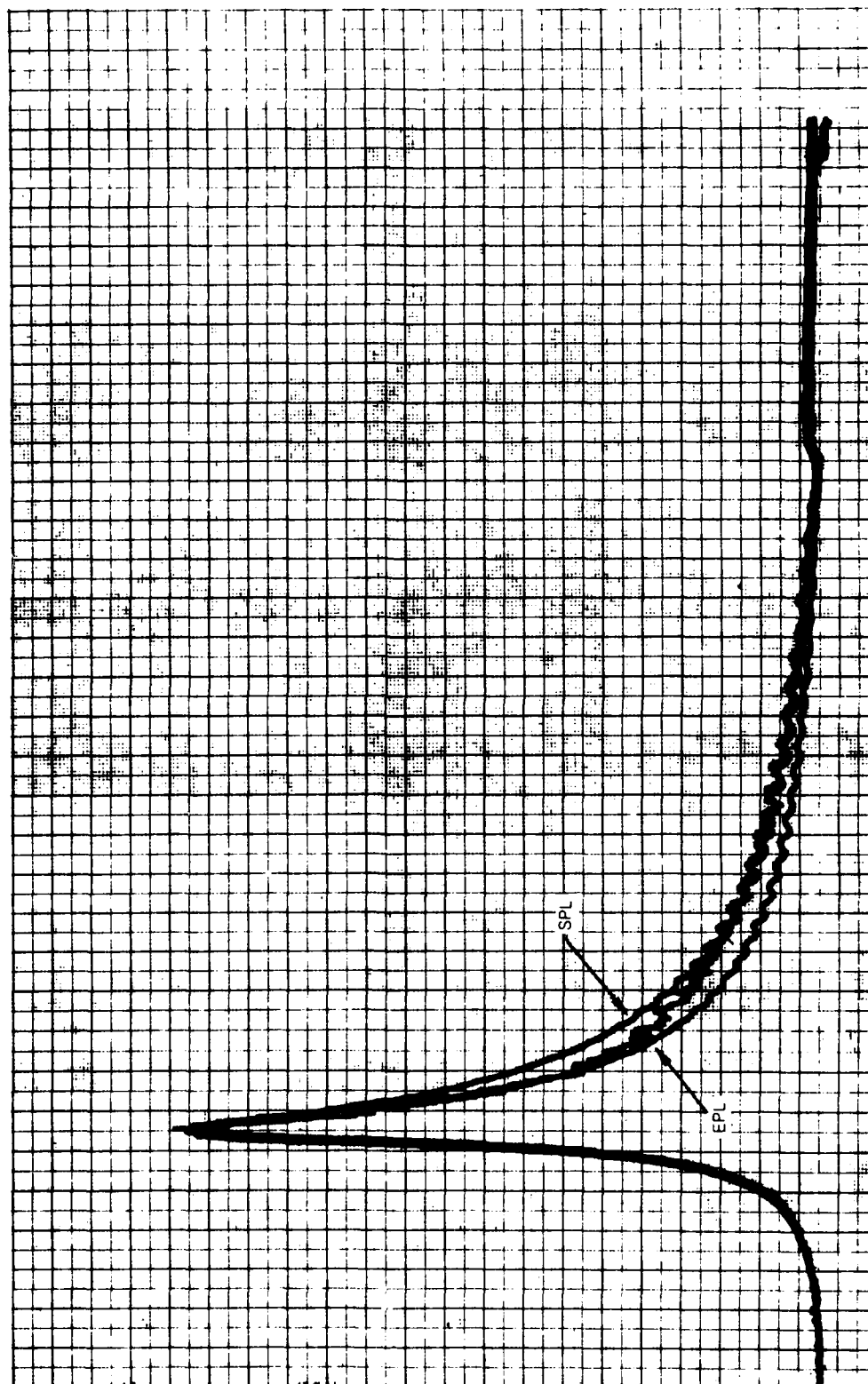
COMPARISON BETWEEN THEORY AND EXPERIMENT — CO CARS

T = 949K   P = 103.7 atm
OVERALL RESOLUTION = 0.47 cm⁻¹

84—1—45—4

35

FIG. 19
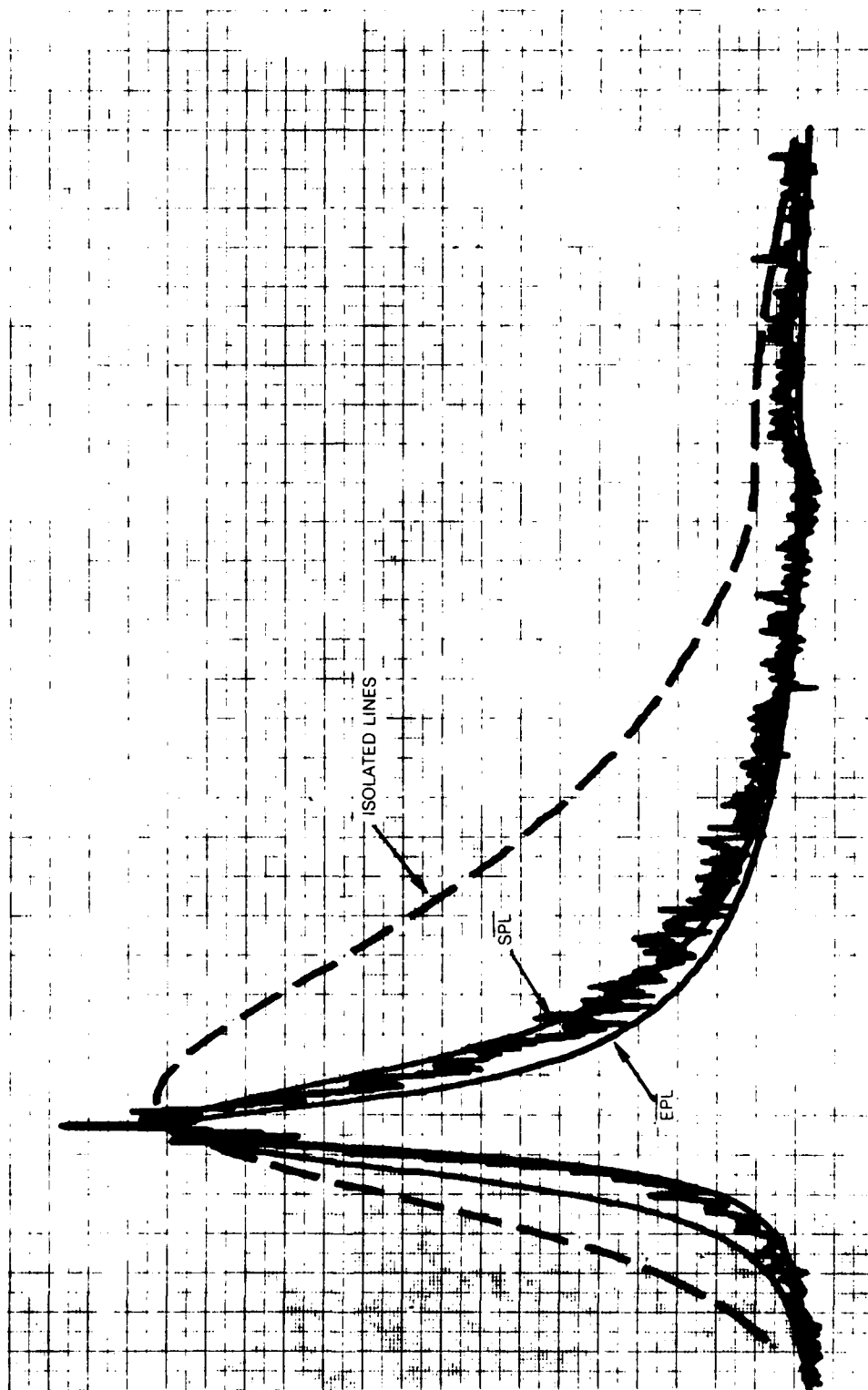
COMPARISON BETWEEN THEORY AND EXPERIMENT — CO CARS

T = 1555K   P = 10.2 atm

OVERALL RESOLUTION = 0.47 cm^{-1}

84-1-45-9A

36

FIG. 20
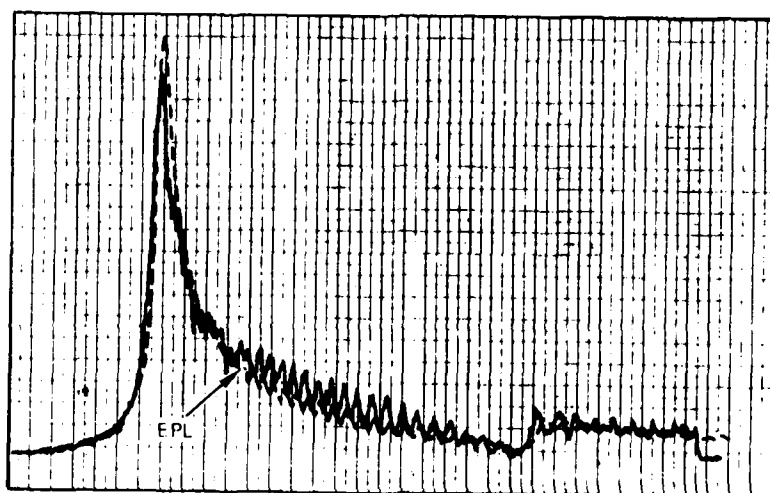
COMPARISON BETWEEN THEORY AND EXPERIMENT — CO CARS

T = 1528K   P = 82.6 atm
OVERALL RESOLUTION = 0.47 cm⁻¹
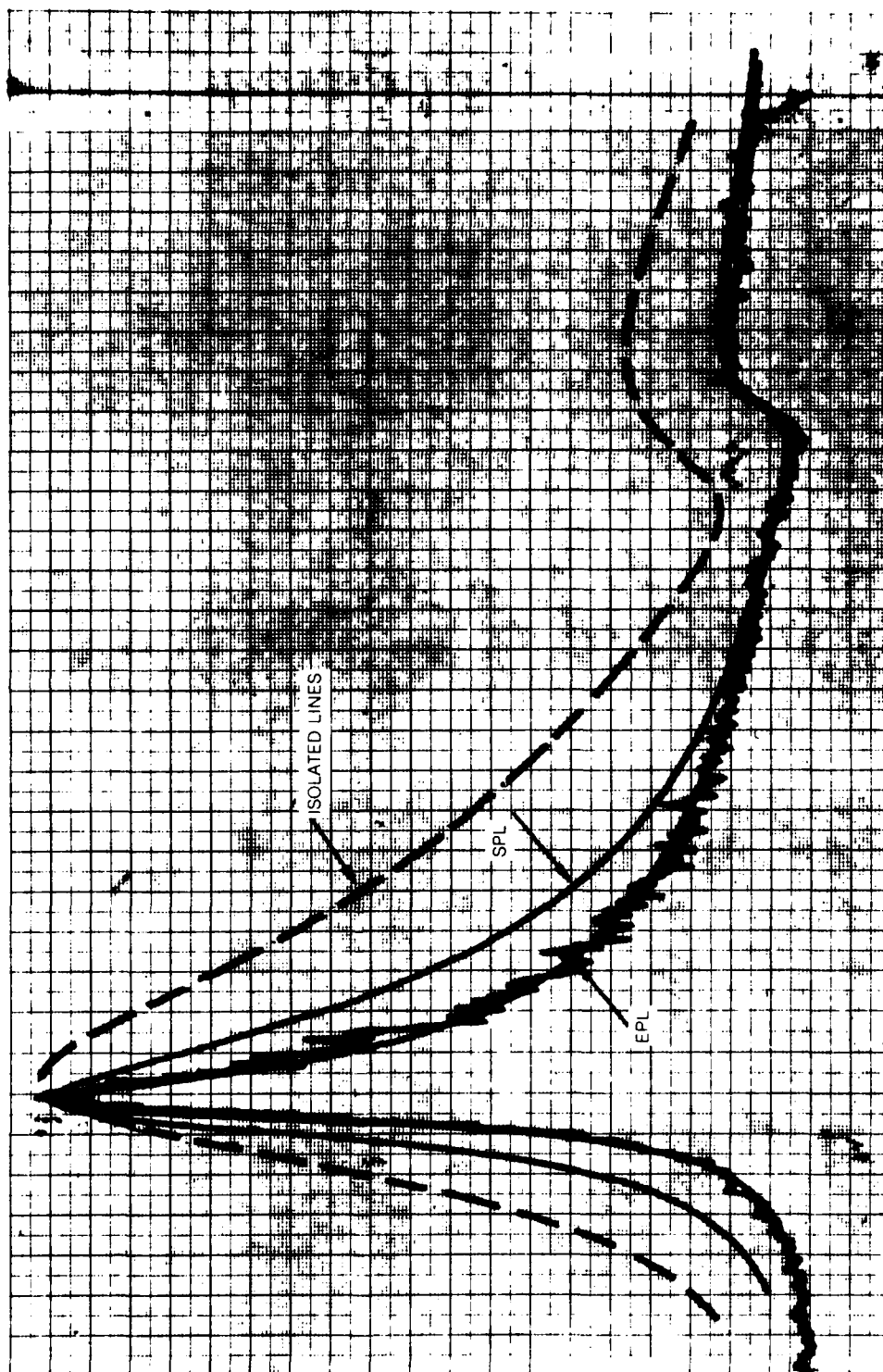
84–1–45–10

N_2 (Ref. 27). The investigations undertaken in this contract represent
quite an extensive test of the basic theory of high pressure CARS, and it
is encouraging that such good results can be obtained from linewidth models
of such simple form. The diagnostic implications of the work completed
under the current contract are encouraging. Based on the results of these
pure CO investigations, it is expected that minority species CO spectra
will also be successfully interpreted by the collisional narrowing model.

AREAS OF FUTURE WORK

The successful completion of the tasks in this current contract have resulted in verification of the ability of the UTRC CARS computer code to accurately model and predict the CARS spectrum of carbon monoxide over the temperature range 300K-1500K and for pressures from 1-100 atm. The code now represents a powerful tool for accurate temperature and concentration measurements of this molecule in combustion media. A logical extention of the current work is to proceed with experiments in high pressure laboratory flames, (i.e. CO/air) and attempt flame chemistry studies through CARS measurements of temperature and species concentration in high pressure flame environments.

REFERENCES

1. Nibler, J. W., Shaub, W. M., McDonald, J. R. and Harvey, A. B., "Coherent Anti-Stokes Raman Spectroscopy," in Vibrational Spectra and Structure, Vol. 6, J. R. Durig, Ed., Elsevier, Amsterdam, 1977, pp. 173-225.

2. Eckbreth, A. C. and Schreiber, P. W., "Coherent Anti-Stokes Raman Spectroscopy (CARS): Application to Combustion and Gas-Phase Diagnostics," in Chemical Applications of Nonlinear Raman Spectroscopy, A. B. Harvey, Ed., Academic Press, New York, 1981, pp. 27-87.

3. Eckbreth, A. C., "BOXCARS: Crossed-Beam Phase-Matched CARS Generation in Gases," Applied Physics Letters, Vol. 32, 1978, pp. 421-423.

4. Eckbreth, A. C., Dobbs, G. M., Stufflebeam, J. H., and Tellex, P. A., "CARS Temperature and Species Measurements in Augmented Jet Engine Exhausts," AIAA Paper No. 83-1294, Presented at the AIAA/ASME/SAE 19th Joint Propulsion Conference, Seattle, Washington, June, 1983. To appear in Applied Optics, 1984.

5. Eckbreth, A. C. and Hall, R. J., "CARS Thermometry in a Sooting Flame," Combustion and Flame, Vol. 36, 1979, pp. 87-98.

6. Eckbreth, A. C. and Hall, R. J., "CARS Concentration Sensitivity with and Without Nonresonant Background Suppression," Combustion Science and Technology, Vol. 25, 1981, pp. 175-192.

7. Druet, S. A. J., and Taran, J. P. E., "CARS Spectroscopy," Progress in Quantum Electronics, Vol. 7, 1981, pp. 1-72.

8. Nibler, J. W. and Knighten, G. V., "Coherent Anti-Stokes Raman Spectroscopy," in Raman Spectroscopy of Gases and Liquids, A. Weber, Ed., Springer-Verlag, Berlin, 1979, pp. 253-299.

9. Hall, R. J. and Eckbreth, A. C., "Coherent Anti-Stokes Raman Spectroscopy (CARS): Application to Combustion Diagnostics," to appear in Laser Applications Vol. V, R. K. Erf, Ed., Academic Press, New York. (1984).

10. Baranger, M., "Problem of Overlapping Lines in the Theory of Pressure Broadening," Physical Review, Vol. 111, 1958, pp. 494-504.

11. Kolb, A. C., and Griem, H., "Theory of Line Broadening in Multiplet Spectra," Physical Review, Vol. 111, 1958, pp. 514-521.

12. Gordon, R. G., "On the Pressure Broadening of Molecular Multiplet Spectra," Journal of Chemical Physics, Vol. 46, 1967, pp. 448-455.

13. Alekseyev, V. et al., "Stimulated Raman Scattering in Gases and Gain Pressure Dependence," IEEE Journal of Quantum Electronics, Vol. QE-4, 1968, pp. 654-656.A.

14. Hall, R. J., Verdieck, J. F., and Eckbreth, A. C., "Pressure-Induced Narrowing of the CARS Spectrum of N_2," Optics Communications, Vol. 35, 1980, pp. 69-75.

15. Brunner, T. A., Pritchard, D., "Fitting Laws for Rotationally Inelastic Collisions," in Advances in Chemical Physics, Dynamics of the Excited State, John Wiley, New York, 1982.

16. Polanyi, J. C. and Woodall, K. B., "Mechanism of Rotational Relaxation," Journal of Chemical Physics, Vol. 56, 1972, pp. 1563-1572.

17. Stufflebeam, J. H., Hall, R. J., and Verdieck, J. F., "CARS Diagnostics of High Pressure and Temperature Gases," Paper No. 83-1478 presented at 18th AIAA Thermophysics Conf. Montreal, Canada, June 1-3, 1983.

18. Rosasco, G. J. et al., "Line Interference Effects in the Vibrational Q-Branch Spectra of N_2 and CO," Chemical Physics Letters, Vol. 97, 1983, p. 435.

19. Gordon, R. G., "On the Rotational Diffusion of Molecules," Journal of Chemical Physics, Vol. 44, 1966, pp. 1830-1836.

20. Brueck, S. R. J., "Vibrational Two-Photon Resonance Linewidths in Liquid Media," Chemical Physics Letters, Vol. 50, 1977, pp. 516-520.

21. Hall, R. J. and Greenhalgh, D. A., "Application of the Rotational Diffusion Model to Gaseous N_2 CARS Spectra, Optics Communications, Vol. 40, 1982, pp. 417-420.

22. Papineau, N., and Pealat, M., "Numerical Simulation of the Coherent anti-Stokes Raman Scattering Spectrum of CO_2," Journal of Chemical Physics, Vol. 79, 1983, pp. 5758-5768.

23. BelBruno, J. J., Gelfand, J., and Rabitz, H., "Collision Dynamical Information from Pressure Broadening Measurements: Application to Carbon Monoxide," Journal of Chemical Physics, Vol. 78, 1983, pp. 3990-3998.

24. Sun, J. N. P., and Griffiths, P. R., "Temperature Dependence of the Self-Broadening of Coefficients for the Fundamental Band of Carbon Monoxide," Applied Optics, Vol. 20, 1981, pp. 1691-1695.

25. Varghese, P. L., and Hanson, R. K., "Tunable Infrared Diode Laser Measurement of Strengths and Collisional Widths of CO at Room Temperature," Journal of Quantitative Spectroscopy and Radiative Transfer, Vol. 24, 1980, pp. 479-489.

26. Varghese, P. L., and Hanson, R. K., "Collision Width Measurements of CO in Combustion Gases Using a Tunable Diode Laser," Journal of Quantitative Spectroscopy and Radiative Transfer, Vol. 26, 1981, pp. 339-348.

27. Hall, R. J., "Pressure-Broadened Linewidths for N_2 Coherent Anti-Stokes Raman Spectroscopy Thermometry," Applied Spectroscopy, Vol. 34, 1980, pp. 700-701.

28. Dexheimer, S. L. et al., "Dynamical Constraints on the Transfer of Angular Momentum in Rotationally Inelastic Collisions of I_2 with He and Xe," Journal of Chemical Physics, Vol. 76, 1982, pp. 4996-5004.

29. Matheson Gas Data Book, Fourth Ed., The Matheson Company, Inc., East Rutherford, New Jersey, 1966, p. 94.

30. Marko, K. A. and Rimai, L., "Space- and Time-Resolved Coherent Anti-Stokes Raman Spectroscopy for Combustion Diagnostics," Optics Letters, Vol. 4, 1979, pp. 211-213.

31. Davis, L. C., Marko, K. A., and Rimai, L., "Angular Distribution of Coherent Raman Emission in Degenerate Four-Wave Mixing with Pumping by a Single Diffraction Coupled Laser Beam: Configurations for High Spatial Resolution," Applied Optics, Vol. 20, 1981, pp. 1685-1690.

32. St. Peters, R. L., "Augmented Coherent Anti-Stokes Raman Spectroscopy Linewidth Parameter from Laser-Mode Structure," Optics Letters, Vol. 4, 1979, pp. 401-402.

33. Koszykowski, M. L., "The J Dependence of N_2 Vibrational Spectra," Unpublished results. Rahn, L. A., Owyoung, A., Coltrin, M. E., and Koszykowski, M. L., "The J Dependence of Nitrogen 'Q' Branch Line-widths," Proceedings of the VIIth International Conference on Raman Spectroscopy, Ottawa, Canada, W. R. Murphy, Editor, 1980, pp. 694-695.

APPENDIX

EXPERIMENTAL CARBON MONOXIDE CARS SPECTRA

0.47 cm^{-1} Resolution

1.0 atm.

295K

1 cm^{-1}

28.9 atm.

295K

$\vdash$ 1 cm^{-1}

58.8 atm.

295K

— 1 cm^{-1}

79.2 atm.

295K

1 cm⁻¹

1.0 atm.

689K

$1\ cm^{-1}$

10.2 atm.

736K

1 cm⁻¹

R83-956020-F

A-11

9.8 atm.

971K

1 cm^{-1}

A-12

103.7 atm.

949K

1 cm^{-1}

1.0 atm.

1265K

$\leftarrow$ 1 cm^{-1}

7.1 atm.

1247K

— 1 cm^{-1}

10.2 atm.

1250K

1 cm^{-1}

10.2 atm.

1555K

$\vdash$ 1 cm^{-1} $\dashv$

82.6 atm.

1528K

$1\ cm^{-1}$